Available online at www.sciencedirect.com
ScienceDirect
Developmental Biology 314 (2008) 171–188
DEVELOPMENTAL BIOLOGY
www.elsevier.com/developmentalbiology

Altered neuronal lineages in the facial ganglia of *Hoxa2* mutant mice

Xiu Yang [a,1], Yuefang Zhou [b,1], Erin A. Barcarse [a], Stephen O'Gorman [a,*]

[a] *Department of Neurosciences, Case Western Reserve University, School of Medicine, 10900 Euclid Avenue, Cleveland, OH 44106, USA*
[b] *Department of Neurology and Psychiatry, Saint Louis University, 1438 S. Grand Blvd., St Louis, MO 63110, USA*

Received for publication 28 June 2007; revised 24 October 2007; accepted 21 November 2007
Available online 31 December 2007

Abstract

Neurons of cranial sensory ganglia are derived from the neural crest and ectodermal placodes, but the mechanisms that control the relative contributions of each are not understood. Crest cells of the second branchial arch generate few facial ganglion neurons and no vestibuloacoustic ganglion neurons, but crest cells in other branchial arches generate many sensory neurons. Here we report that the facial ganglia of *Hoxa2* mutant mice contain a large population of crest-derived neurons, suggesting that *Hoxa2* normally represses the neurogenic potential of second arch crest cells. This may represent an anterior transformation of second arch neural crest cells toward a fate resembling that of first arch neural crest cells, which normally do not express *Hoxa2* or any other Hox gene. We additionally found that overexpressing *Hoxa2* in cultures of P19 embryonal carcinoma cells reduced the frequency of spontaneous neuronal differentiation, but only in the presence of cotransfected Pbx and Meis Hox cofactors. Finally, expression of Hoxa2 and the cofactors in chick neural crest cells populating the trigeminal ganglion also reduced the frequency of neurogenesis in the intact embryo. These data suggest an unanticipated role for Hox genes in controlling the neurogenic potential of at least some cranial neural crest cells.

Keywords: *Hoxa2*; Cranial ganglia; Lineage marking; Neural crest; Neurogenesis; Hox genes; P19 cells; Pbx; Meis

Introduction

The sensory neurons of cranial nerve ganglia are mosaic populations that include neurons generated by ectodermal placodes and by neural crest cells in successive stages (Ayer-LeLievre and LeDouarin, 1982; d'Amico-Martel and Noden, 1983). There are large and reproducible variations in the relative numbers and positions of placode-derived and crest-derived neurons in specific cranial ganglia. Whereas the trigeminal ganglion contains many crest-derived neurons, the vestibuloacoustic ganglion contains none and the facial ganglion contains very few. Placode- and crest-derived neurons associated with the glossopharyngeal and vagal nerves are physically segregated into distal (petrosal and nodose) and proximal (jugular and superior) ganglia. The mechanisms that lead to these variations have not been identified.

Manipulations that remove placode-derived neurons have shown that cranial neural crest cells generate additional neurons when placode-derived neurons are missing (Fode et al., 1998; Harrison et al., 1995). A similar regulation of neurogenic potential has been observed between early- and late-migrating populations of neural crest cells in zebrafish dorsal root ganglia (Raible and Eisen, 1996), and between *Neurogenin2*- (*Neurog2*) and *Neurogenin1*- (*Neurog1*) dependent neurons of mammalian dorsal root ganglia (Ma et al., 1999). Cranial neural crest cells that do not normally form neurons, such as those of the nodose ganglion, can generate neurons upon transplantation to appropriate environments (Ayer-LeLievre and LeDouarin, 1982). Such observations have led to the suggestion that the presence of placode-derived neurons normally represses neurogenesis by cranial neural crest cells (Ayer-LeLievre and LeDouarin, 1982).

Differences in the numbers of crest-derived neurons may, additionally or alternatively, reflect differences in the developmental potential of crest cells themselves. Many non-neuronal fates of cranial neural crest cells are modulated by the activities of Hox genes (Couly et al., 2002). A striking example is the

* Corresponding author. Fax: +1 216 368 4650.
E-mail address: ogorman@case.edu (S. O'Gorman).
[1] These authors made equal contributions to the manuscript.

0012-1606/$ - see front matter © 2007 Elsevier Inc. All rights reserved.
doi:10.1016/j.ydbio.2007.11.032

requirement for *Hoxa2* function in neural crest cells that arise from the fourth rhombomere (r4) of the hindbrain and form the mesenchyme of the second branchial arch. Loss of *Hoxa2* function results in neonatal lethality and the transformation of some second arch skeletal elements toward fates normally assumed by first arch neural crest cells (Gendron-Maguire et al., 1993; Rijli et al., 1993). The phenotype is similar to that observed after heterotopic transplantation of the neuroepithelium that normally gives rise to first arch neural crest into sites that give rise to second arch neural crest (Noden, 1983). Additionally, ectopic expression of *Hoxa2* in the first branchial arch leads to alterations of crest cell fate that are consistent with a loss of first arch identity (Creuzet et al., 2002; Grammatopoulos et al., 2000). *Hoxa2* thus appears to actively promote development of second arch skeletal elements and connective tissues from crest-derived mesenchyme. Whether *Hoxa2*, or indeed any Hox gene, contributes to the control of neurogenesis by neural crest cells within developing cranial ganglia is not known.

In this study, we have used a lineage marking paradigm based on the transient expression of a site-specific recombinase (O'Gorman et al., 1991) to heritably label the second arch neural crest cell lineage. As previously described by others (Arenkiel et al., 2003), we found that in wild-type embryos the neural crest population that arises from *Hoxb1*-expressing progenitors in r4 preferentially formed glial cells in the facial ganglion, but we also found that it formed a small number of sensory neurons in the facial ganglion and all of the parasympathetic neurons of the ptergopalatine ganglion. Unexpectedly, we found that in mutant embryos lacking *Hoxa2* function, the r4-derived neural crest cells generated a large, supernumerary population of facial ganglion neurons, suggesting that *Hoxa2* function normally represses neurogenesis in this population of neural crest cells. This hypothesis was tested by overexpressing Hoxa2 in high-density cultures of P19 embryonal carcinoma cells (Jones-Villeneuve et al., 1982; Rudniki and McBurney, 1987). Coexpression of *Hoxa2*, along with *Pbx* and *Meis* cofactors, reduced the probability of neuronal differentiation in these experiments, an effect that could be antagonized by simultaneous expression of a Hox3 paralogue. Finally, in ovo electroporation was used to express Hoxa2 and the cofactors in neural crest cells that enter the trigeminal ganglion, which normally generate both neurons and glia. We found that the frequency with which transfected cells differentiated as neurons was significantly reduced. Collectively, these data demonstrate that the commitment of pluripotent cells to neuronal and non-neuronal fates may be influenced by the activity of Hox genes and their cofactors.

Materials and methods

Mice

The *Hoxb1* locus was isolated from a 129 strain genomic lambda phage library (Stratagene) using a cDNA probe (Frohman et al., 1990). A targeting vector (Fig. 1A) was prepared that contained a Cre recombinase coding sequence from pOG231 (O'Gorman et al., 1997), a neomycin resistance cassette from pMC1neo-polyA (Thomas and Capecchi, 1987), and a HSV thymidine kinase cassette from pNT (Tybulewicz et al., 1991). Linearized vector was transfected into CCE embryonic stem cells (Robertson et al., 1986) and recombinant clones were isolated by selection with G418 and ganciclovir and identified by Southern blotting (Fig. 1B). Germline transmission of two independent clones was obtained; both recombinant alleles had phenotypes that were the same as reported null alleles (Goddard et al., 1996; Studer et al., 1996) and behaved as simple Mendelian recessives. The mutant alleles were backcrossed onto a B6D2F1 background. Mice with a null allele of *Hoxa2* (*hoxa2*^{tm1Grid}; Gendron-Maguire et al., 1993) were obtained from Jackson Laboratories. Mice bearing the Cre-conditional *R26R* reporter allele (Soriano, 1999) were obtained from Philippe Soriano. Mice bearing a null allele of the *Bdnf* locus (Conover et al., 1995) were obtained from David Katz. Each strain was maintained by backcrossing to B6D2F1 hybrids. For timed pregnancies, the day of vaginal plugging was designated E0.5. Embryos were harvested into cold PBS and fixed in 4% phosphate-buffered formaldehyde for 1–4 h, washed in PBS, and either stored in methanol for whole mount in situ hybridization or equilibrated with 30% sucrose in PBS for frozen sectioning for immunohistochemistry or in situ hybridization.

Expression constructs

Expression plasmids for GFP (pUS2-GFP), *Neurogenin1* (pCS2-Ngn1), *NeuroD2* (pUS2-NeuroD2) (McCormick et al., 1996), and puromycin (pUS2-puro) were generously provided by Dr. David Turner. Expression plasmids for Hoxa2 (pCMV-Hoxa2), Pbx1 (pCMV-Pbx1), and Meis1 (pCMV-Meis1) were prepared by amplifying the respective coding sequences from a mouse cDNA library (*Clonetech*) and cloning the products into pCDNA3.1 (*Invitrogen*). The pCMV-Hoxd3 expression plasmid was generously provided by Nancy Boudreau (Boudreau et al., 1997). pUS2-Neurog1 was made by shuttling the I sequence from pCS2-Ngn1 into pUS2. A plasmid expressing a mutant Hoxa2 (W99A) protein unable to heterodimerize with Pbx proteins was prepared by using a mutagenesis kit (Quikchange, Stratagene) to change the conserved tryptophan residue of the pentapeptide sequence (Knoepfler and Kamps, 1995) to alanine. The resulting plasmid was fully sequenced to confirm that only the desired change occurred.

Neuronal differentiation assays using P19 cells

P19 cells were maintained at subconfluent densities in alpha MEM with 7.5% calf serum and 2.5% fetal bovine serum (FBS, Gibco) (Rudniki and McBurney, 1987). Twenty-four hours before transfection, aliquots of 2×10^5 cells were plated in 6 cm dishes. In the first series of experiments, P19 cells were transfected with pUS2-GFP and various combinations of expression plasmids for *Hoxa2*, *Hoxd3*, *Pbx1*, *Meis1*, and *Neurog1*. Each transfection included 2 μg of one to four expression plasmids, 2 μg of pUS2-GFP, and enough neutral vector (pUS2-puro) to bring the total amount of plasmid DNA to 10 μg in FuGene6 transfection reagent (*Roche*). After overnight incubation, cells were resuspended and seeded on gelatin-coated cover-slips in 24-well plates (2×10^4 cells per well) and 24 h later the medium was changed to Opti-MEM with 1% FBS to promote differentiation. The medium was changed after a further two days and the cells were fixed and stained with antibodies to PGP9.5 (Wilkinson et al., 1989) after a total of 4 days in differentiation medium. Given the low frequencies of neuronal differentiation seen in most of these transfections, neuronal differentiation was scored as the fraction of PGP9.5-positive neurons that arose from transfected (GFP-positive) cells. Because neuronal differentiation was efficiently induced by Neurog1, neurogenesis in transfections that included the Neurog1 expression plasmid was scored as the fraction of GFP-positive cells that were also PGP9.5 positive.

In a second series of experiments, a test population of P19 cells was seeded onto feeder layers of P19 cells that had been transfected with a combination of *Hoxa2*, *Pbx1*, and *Meis1* expression plasmids (see timeline in Supplementary Fig. 1). The feeder cells were transfected on day 1 as described above (omitting the GFP expression plasmid), mitotically inactivated 24 h later using MitomycinC, and then seeded at a density of 6×10^5 cells per well on gelatinized coverslips in 24-well plates (day 2). The test population of P19 cells was transfected with pUS2-GFP on day 2, and was resuspended and plated on the feeder cells at a density of 3000 cells per well in Opti-MEM with 1% FBS on day 3. The cultures were maintained with daily changes of medium for a further 4 days before being fixed and labeled for scoring. In these experiments, neuronal

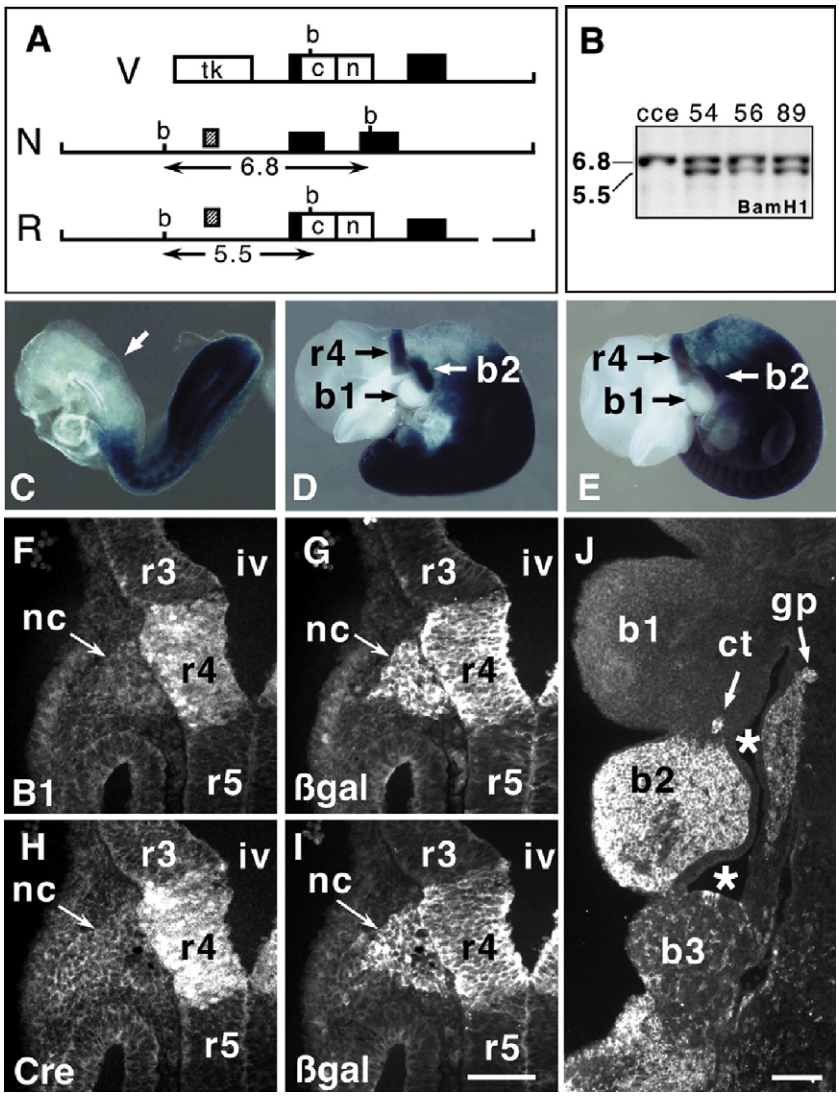

Fig. 1. Structure and activity of $B1^{Cre}$ allele. (A) Vector (V), native *Hoxb1* locus (N), and recombinant $B1^{Cre}$ allele (R). The targeting vector contained (5′ to 3′) an HSV thymidine kinase cassette (tk), 1.8 kb of *Hoxb1* genomic sequence, a Cre coding sequence (c), a neomycin cassette (n), and 10.5 kb of genomic sequence. *Hoxb1* exons are shown as black rectangles, *Bam*HI (b) endonuclease sites and the sizes (kb) of the fragments generated are indicated. (B) Southern blots of *Bam*HI-digested DNA from wild-type (cce) embryonic stem cells and three recombinant clones (54, 56, 89) probed with an external probe (hatched box in panel A). Other digestions and probes confirmed the organization of the recombinant clones (not shown). (C) Histochemical staining of $+/B1^{Cre}$, +/*R26R* (*Hoxa2* +/+) embryo at E8.5 showed marker expression in the presumptive r4 domain (arrow). (D, E) Staining of E9.5 $+/B1^{Cre}$ (D) and $B1^{Cre}/B1^{Cre}$ (E) embryos (also +/*R26R, Hoxa2* +/+) showing marker expression in r4 and the second branchial arch (b2) and the absence of product in the first arch (b1). $B1^{Cre}/B1^{Cre}$ embryos showed increased labeling of posterior hindbrain and third arch. (F–I) Horizontal sections (anterior to the top, midline to the right) of an E9.5 $+/B1^{Cre}$, +/*R26R* (*Hoxa2* +/+) embryo. (F, H) Adjacent sections showing Hoxb1 (F) and Cre (H) expression in r4, lack of expression in r3 and r5, and sharply reduced expression in r4-derived neural crest cells (nc) (iv, fourth ventricle). (G, I) Sustained marker expression in the neural crest in the sections shown in F and H, respectively. (J) Sagittal section (dorsal to right and anterior at top) of an E10.5 *Hoxa2* +/+, $+/B1^{Cre}$, and +/*R26R* embryo showing labeling of second arch mesenchyme, including cells dorsal to the pharyngeal cavity (*), lack of first arch labeling, and low level of labeling in the third arch (b3). (ct: chorda tympani, gp: greater petrosal nerve) Scale bars: I, 50 μm for panels panels F–I; J, 100 μm.

differentiation was scored as the fraction of GFP-positive cells that had differentiated as neurons (PGP9.5-positive).

In ovo electroporation

In ovo electroporations were done on HH stage 10 (Hamburger and Hamilton, 1952) chick embryos. Expression plasmids were mixed in PBS containing Trypan blue and pressure-injected into the lumen of the neural tube just posterior to the midbrain vesicles. All injection mixes contained 4 μg/μl of a CMV-GFP expression plasmid, various combinations of Hoxa2, Pbx1, and Meis1 expression plasmids (each at 1.5 μg/μl), and enough empty CMV expression vector to bring the total plasmid concentration to 8.5 μg/μl for each mix. Electroporation was performed using an BTX electroporator (ECM 830) delivering five 50 ms square pulses of 18 V through platinum electrodes placed on either side of the neural tube at the midbrain level. Transfected embryos were allowed to develop for 4 days and then examined under fluorescent illumination using a Zeiss dissecting microscope. Embryos expressing GFP in trigeminal ganglia were fixed and processed for immunohistochemistry.

Immunohistochemistry

Sections or coverslips were blocked with 5% normal donkey serum in PBST (PBS plus 0.3% triton) and primary antibodies were applied overnight at 4 °C. Primary antibodies included goat anti b-galactosidase (Biogenesis, 1:3000); rabbit anti b-galactosidase (Cappel, 1:5000); mouse anti b-tubulin (Tuj1) (Babco, 1:1000) (Lee et al., 1990); rabbit anti neurofilament 200 (Sigma,

1:3000); rabbit anti PGP 9.5 (Accurate, 1:20,000) (Wilkinson et al., 1989); mouse anti-Islet1/2 (Developmental Studies Hybridoma Bank, 1:100) (Ericson et al., 1992); rabbit anti TrkA (Chemicon, 1:500); rabbit anti phosphohistone H3 (Upstate, 1:800); and mouse anti Sox10 (Lo et al., 2002). Secondary antibodies (Jackson Immunochemicals) conjugated to either Cy3 or FITC were applied for 2 h. Histological material generated from mouse embryos was examined and photographed with a Zeiss Axioskop microscope equipped with a Hamamatsu digital camera, while sections of electroporated chick embryos were photographed using a Zeiss LSM410 confocal microscope.

In situ hybridization

The probes for mouse *Delta-like1* (*Dll1*; Bettenhausen et al., 1995), mouse *Delta-like3* (*Dll3*; Dunwoodie et al., 1997), and *Notch1* (Conlon et al., 1995) were provided by Ronald Conlon. The second exon of *Hoxa2* and the entire *Neurog1* and *Neurogenin2* (*Neurog2*) coding sequences were amplified by PCR from genomic DNA, cloned into pCR4-TOPO (Invitrogen), and their identities were confirmed by sequencing. Digoxigenin-labeled sense and antisense probes were synthesized using a kit (*Roche*) according to the manufacturer's instructions. Hybridization was performed as described by Schaeren-Wiemers and Gerfin-Moser (1993).

Quantification

For sectioned material, cell counts were made on every fourth, 15 μ thick frozen section from serial sets through the facial and vestibuloacoustic ganglia of E14.5 embryos. Singly PGP9.5-positive cellular profiles and doubly PGP9.5- and β-galactosidase marker-positive profiles were counted separately without correction for nuclear size. The volumes of ganglia were determined using Openlab software. The data presented represent counts from both ganglia of three wild-type and three mutant embryos that were then averaged. For the first series of P19 cell transfections, coverslips were scanned in a predetermined, orthogonal pattern. All fields containing PGP9.5-positive neuronal profiles were photographed until at least 200 cells had been sampled, and the number of PGP9.5-positive cells that coexpressed GFP was determined. For the feeder cell experiment and the *Neurog1* transfections, coverslips were scanned in the same manner, all fields containing GFP-positive cells were photographed until a total of 200 cells had been sampled, and the number of GFP-positive cells that coexpressed PGP9.5 was determined. All transfection assays were repeated three times. For quantification of neurogenesis in chick embryos, approximately 100 GFP-positive cells were scored for nuclear Islet1/2 expression in at least three embryos for each plasmid combination.

Results

Labeling of r4 and r4-derived neural crest by the $B1^{Cre}$ allele

To mark the neural crest that populates the second branchial arch for lineage analysis, we prepared a recombinant allele of *Hoxb1* ($B1^{Cre}$) in which the first exon was replaced by the coding sequence for Cre recombinase (Materials and methods, Figs. 1A, B). This allele was null for *Hoxb1* expression (not shown) and was predicted to express Cre in tissues that normally express *Hoxb1*. Cre-mediated recombination of a Cre-conditional reporter allele would be expected to heritably label the lineages that descend from *Hoxb1*-expressing progenitors. The expression pattern of *Hoxb1* is highly dynamic (Frohman et al., 1990; Murphy et al., 1989). At early stages (embryonic day 7.5 (E7.5)), it is expressed in the posterior primitive streak and flanking mesoderm. By E8.5, expression is observed in the neural tube up to the presumptive r3/4 boundary in the hindbrain, and is elevated in r4 itself. Between E8.5 and E9.5, *Hoxb1* expression is increases in r4 but rapidly decreases in more caudal regions of the hindbrain. Based on this expression pattern, the $B1^{Cre}$ allele could potentially label all cells derived from rhombomere 4, including the r4-derived neural crest cells that enter the second branchial arch.

In $+/B1^{Cre}$ embryos, the patterns of Hoxb1 protein expression (from the wild-type allele) and Cre recombinase expression (from the B1Cre allele) were identical (Figs. 1F, H, and data not shown). At E9.5, cells in r4 expressed high levels of both proteins. By contrast, both Hoxb1 and Cre proteins were nearly undetectable in neural crest cells that had emerged from r4. This finding is consistent with reports that *Hoxb1* mRNA is not expressed in r4-derived neural crest (Frohman et al., 1990; Murphy and Hill, 1991). We were unable to detect Hoxb1 or Cre protein in more distal cells of the second branchial arch at E9.5 or E10.5, or in any craniofacial tissues or the hindbrain at E11.5, E12.5, E15.5, or P0 (not shown). We never observed either Hoxb1 or Cre expression in the neural tube rostral to r4.

In embryos containing the $B1^{Cre}$ allele and the Cre-conditional R26R β-galactosidase marker allele (Soriano, 1999) ($+/B1^{Cre}$; *+/R26R*), β-galactosidase expression from the recombined marker allele could be observed in the presumptive r4 territory as early as E8.75 (Fig. 1C). By E9.5, all cells in r4 expressed the marker (Figs. 1D, G, I). By contrast, no marker expression was observed in neural tissues anterior to r4, and only low levels of marker activation were seen in more posterior rhombomeres. The labeling of the posterior hindbrain is likely to result from the transient expression of Hoxb1 and Cre prior to approximately E9. Considerably more recombination in r5 and the posterior hindbrain was seen in embryos homozygous for the $B1^{Cre}$ allele (Fig. 1E). In these embryos, r4 was still completely labeled, despite the fact that Hoxb1 positively regulates its own expression (Popperl et al., 1995).

At E10.5, the territory expressing the marker extended from the root of the facial nerve to the distal extremity of the second branchial arch and included virtually all second arch mesenchymal cells (Figs. 1J, 2A). Temporally, neural crest cells populate the branchial arches in a distal to proximal order, suggesting that the marker was recombined in the first neural crest cells to emerge from r4. The central mesodermal core, which could be identified by the expression of either MyoD (not shown) or Islet1/2 proteins (Fig. 2A), did not express the marker. The surface ectoderm, including the neurogenic ectodermal placode, was also negative for marker expression (Fig. 2B). Unlabeled, Islet1/2-positive cells were positioned between the placode and the developing facial ganglion; these were likely to be neuroblasts that had recently delaminated from the placode that were migrating toward the ganglion (Fig. 2B).

In summary, Cre expression from the $B1^{Cre}$ allele led to recombination of the R26R allele and β-galactosidase expression in all cells of r4 by E9.5, and resulted in marker expression by the r4-derived neural crest cell lineage, including at least most of the earliest r4-derived crest to emerge from the hindbrain. Our immunohistochemical data confirmed observations made by others using in situ hybridization that suggest that *Hoxb1* expression is extinguished in craniofacial tissues after approximately E10.5. We have additionally been unable to

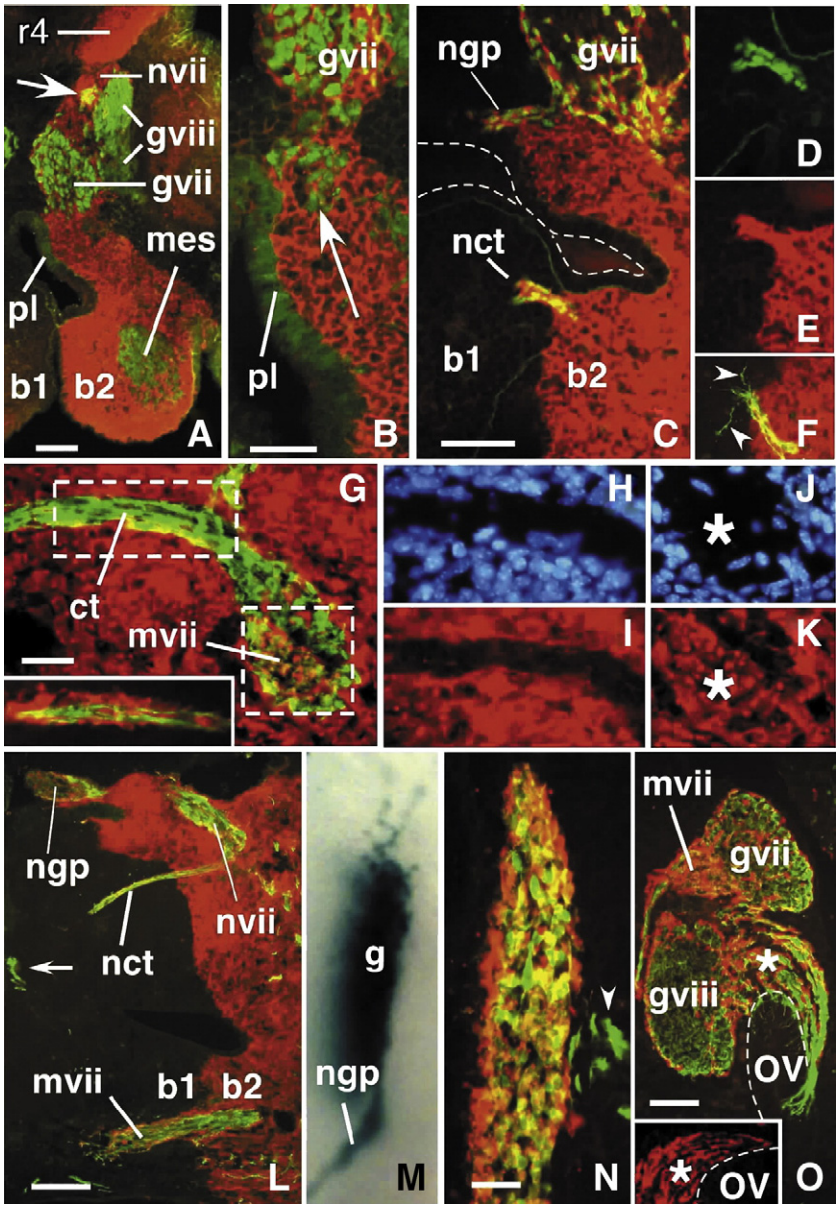

Fig. 2. Marking of second arch tissues by the $B1^{Cre}$ allele in $+/B1^{Cre}$, +/*R26R* (*Hoxa2* +/+) embryos. (A) Sagittal section (dorsal at top and anterior to left) through r4, the facial nerve (nvii) and facial (gvii) and vestibuloacoustic (gviii) ganglia, and the first and second branchial arch (b1, b2) of an E10.5 embryo labeled with antibodies to β-galactosidase (red) and Islet1/2 proteins (green). The mesoderm (mes) and neurons of the ganglia were Islet1/2 positive and marker negative and the ectodermal placode (pl) was faintly positive for Islet proteins. The arrow indicates a cluster of neurons that expressed β-galactosidase. (B) Islet1/2 positive cells (arrow) located between the placode and facial ganglion. (C) Sagittal section of an E10.5 embryo labeled with antibodies to Sox10 (green) and β-galactosidase (red). The early outgrowth of the greater petrosal (ngp) and chorda tympani (nct) nerves included cells that expressed the marker and Sox10. Dotted line outlines pharyngeal cavity. The signals for each antibody in the chorda tympani are shown separately in panels D and E. (F) Earliest outgrowth of chorda tympani in another E10.5 embryo showed isolated axons (arrowheads) labeled with β-tubulin antibody (Tuj1, green). (G) Horizontal section of an E11.5 embryo through the chorda tympani and motor root (mvii) of the facial nerve labeled with antibodies to β-tubulin (green) and β-galactosidase (red). Inset shows an anterior portion of the chorda tympani within the first arch associated with marker-positive cells. (H–K) DAPI stain of cell nuclei (H, J) and immunostaining of β-galactosidase expression (I, K) within the boxes outlined in panel G showing that cells were largely excluded from the axon fascicles of the chorda tympani (H) and motor root (*, J), that the axons of the chorda tympani did not express the marker (I), and that axons of the motor root (*, K) did express the marker. (L) Sagittal section of E14.5 embryo showing that three principal branches of the facial nerve extended from the second arch into the first arch and were accompanied by labeled cells. Arrow indicates axons of a trigeminal nerve branch not associated with labeled cells (nvii, mixed trunk of facial nerve). (M) Histochemical staining of the roof of the oral cavity at E14.5 showing marker expression in the ptergopalatine ganglion (g) and greater petrosal nerve. (N) Sagittal section through the ptergopalatine ganglion of an E13.5 embryo labeled with antibodies to β-galactosidase (red) and PGP9.5 (green) to show double labeling of neurons and marker only labeling of peripheral glial cells. Arrowhead points to trigeminal axons not associated with second arch glial cells. (O) Sensory axons (*) passing from the vestibuloacoustic ganglion to the otic vesicle (ov) were associated with cells that expressed the lineage marker. Inset shows the marker signal alone. Scale bars: A–C, G, 100 μm; L, 200 μm; N, O, 50 μm.

detect Cre expression from the *B1*^{Cre} allele after that stage, and have not observed novel sites of marker expression that cannot be easily traced to the migration of second arch cells in a staged embryo series. We conclude that virtually all of the cells within the second branchial arch territory that express the R26R marker in +/*B1*^{Cre}; +/R26R embryos arise from r4-derived neural crest cells, and that populations that do not express the marker do not arise from r4-derived crest cells.

Labeling of anterior facial nerve branches

The boundary between the mesenchyme of the first and second branchial arches was sharply defined, and through E15 the only marker-expressing cells consistently found anterior to this boundary were associated with branches of the facial nerve (Figs. 2C–O). The greater petrosal nerve branches from the facial nerve trunk immediately distal to the facial ganglion, runs anteriorly above the oropharynx to innervate the ptergopalatine ganglion, and is comprised of preganglionic parasympathetic axons. At E10.5, axons of the nerve had emerged from the second arch territory and were invested with cells that expressed the marker; some of these also expressed Sox10, which labels glial lineages (Kuhlbrodt et al., 1998) (Fig. 2C). At E13.5, the ptergopalatine ganglion was populated by neuronal and non-neuronal cells that expressed the second arch lineage marker (Figs. 2M, N).

A second division of the facial nerve is the chorda tympani, which branches from the facial nerve trunk ventral to the first pharyngeal pouch and contains sensory axons of facial ganglion neurons that innervate lingual taste buds. In some E10.5 specimens, the initial axons of the chorda tympani were observed to cross into first arch mesenchyme without being accompanied by second arch cells (Fig. 2F), but in most E10.5 specimens and at all later stages the nerve was already invested with Sox10-positive cells that coexpressed the marker (Figs. 2C–E, G (inset), L). The axons of the chorda tympani, like their parental cell bodies (see below), did not express the lineage marker (Figs. 2G–I). By contrast, axons of the third major facial nerve branch, its motor root, did express the marker (Figs. 2G, J, K). The motor root exited the second arch territory between E11.5 and E12.5 and was also accompanied by many marker positive second arch cells (Fig. 2L). Labeled second arch cells were also associated with the distal sensory axons of the eighth cranial nerve (Fig. 2O).

r4 neural crest generates few neurons in the facial ganglion of wild-type embryos

At E10.5, only a few of the Islet1/2-positive sensory neurons of the facial ganglia in wild-type embryos expressed the lineage marker (Fig. 3A). Because the ectodermal placode of the second arch did not express the lineage marker while virtually all r4-derived neural crest cells did, and because the placode contributes neurons to the facial ganglion in both birds (Ayer-LeLievre and LeDouarin, 1982; d'Amico-Martel and Noden, 1983) and mice (Fode et al., 1998), we refer to these marker-negative sensory neurons as placodal neurons. Cells expressing the lineage marker and Sox10, a marker of glial precursors (Kuhlbrodt et al., 1998) were scattered throughout the ganglion and ensheathed its external margins (Fig. 3B). At all stages examined (E10.5–E17.5), small clusters of neurons that expressed the lineage marker were consistently found in the proximal ganglion near or within the facial nerve root, and additional labeled neurons were scattered at the periphery of the ganglion (Figs. 3A, C). At E14.5, approximately 6% of facial ganglion neurons expressed the lineage marker (Table 1). The fraction of crest-derived neurons did not appear changed at E17.5 (not shown).

Neural crest-derived neurons in the facial ganglia of Hoxa2 mutant mice

Embryos heterozygous for the *B1*^{Cre} allele and either heterozygous or homozygous for the *hoxa2*^{tm1Grid} null allele did not show changes in the expression of Hoxb1 or Cre at E9.5, when the expression of both in the hindbrain was confined to r4 (not shown). As in wild-type embryos, only faint immunoreactivity for Hoxb1 protein was observed in the ventral portion of r4 at E10.5, and none could be detected in hindbrain or craniofacial tissues at E11.5 or E12.5. This is consistent with previous reports that the expression of the *Hoxb1* allele is not altered in mice lacking *Hoxa2* function (Gendron-Maguire et al., 1993; Rijli et al., 1993; Davenne et al., 1999).

At E10.5, the distribution of placode and crest-derived cells within the facial ganglia of embryos homozygous for the *hoxa2*^{tm1Grid} null allele was similar to that in controls. In both, the majority of Islet1/2-expressing neurons did not express the lineage marker (Figs. 3A, D), and both contained small numbers of marker positive neurons in proximal portions of the ganglion (arrows). By contrast, most Sox10-positive presumptive glial cells did express the marker (Figs. 3B, E), although a few marker-negative glial cells were present in both mutant and wild-type embryos (arrowheads). A consistent and striking difference arose by E11.5, when a substantial number of neurons expressing the lineage marker were present in the proximal ganglion of the mutants (Figs. 3C, F). By E14.5, placode- and crest-derived neurons formed abutting, largely distinct portions of the ganglion (Fig. 3G), and the number of crest-derived neurons in *Hoxa2* mutant embryos exceeded the total number of neurons present in wild-type embryos (Table 1). The emergence of the crest-derived population was not caused by a marked deficiency of placode-derived neurons, which were present in similar numbers in wild-type and mutant embryos (Table 1). Phosphohistone H3 and Islet1/2 labeling showed comparable numbers of mitotically active neuroblasts in E10.5 control and mutant embryos (Figs. 4A, B). Because there was a slight reduction in the number of placode-derived neurons in the sample of *Hoxa2* mutant embryos, and because the complete absence of placode-derived neurons in the facial ganglion has been associated with the delayed generation of sensory neurons, presumably by neural crest, in *Neurog2* mutant embryos (Fode et al., 1998), we asked if reductions of facial ganglion cell number necessarily invoke the production of crest-derived neurons. We therefore combined the *B1*^{Cre} and *R26R* alleles with a

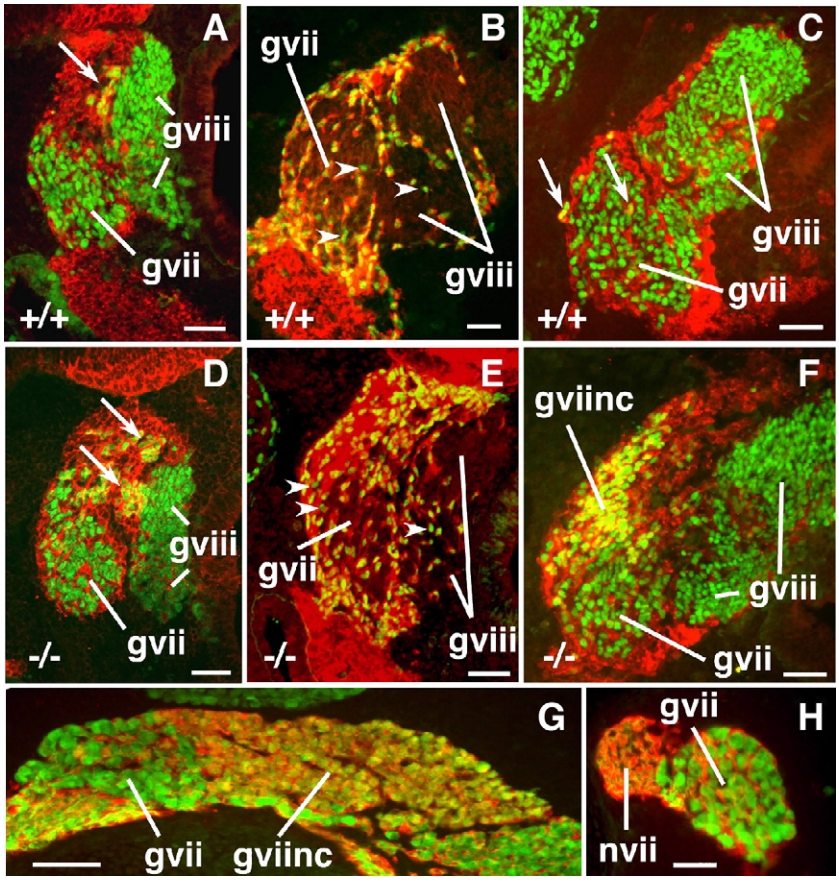

Fig. 3. Facial ganglia of wild-type and *Hoxa2* mutant embryos. β-galactosidase is shown in red in all panels, colabeling with other markers is shown in green. (A–F) Sagittal sections of E10.5 (A, B, D, E) and E11.5 (C, F) wild-type (A–C) and *Hoxa2* mutant (D–F) embryos. (A, D) Islet1/2 colabeling shows the similar organization of facial ganglia in wild-type and mutant embryos at E10.5, both of which contained small numbers of crest-derived neurons in the proximal portion of the ganglion (arrows). (B, E) Sox10 labeling shows that most cells in the glial lineage coexpressed the lineage marker in both mutant and wild-type embryos, although a few cells in each did not (e.g., arrowheads). (C, F) At E11.5, Islet1/2 colabeling shows a few doubly labeled neurons in a wild-type ganglion (arrows, C) and a substantial population of crest-derived neurons (gviinc, F) in the mutant. (G) PGP9.5 colabeling at E14.5 shows a large population of crest-derived neurons (gviinc) in a *Hoxa2* mutant embryo that express both Islet1/2 and the lineage marker: this population was not present in wild-type embryos (see Figs. 4C, D). (H) PGP9.5 colabeling of the facial ganglion of an E14.5 BDNF mutant embryo showed that the neural crest formed few neurons. Scale bars: 50 μm.

null mutation of the *Bdnf* locus (Conover et al., 1995). Although the number of facial ganglion neurons in embryos without *Bdnf* function is reduced by approximately 60% (Jones et al., 1994), examination of serial sections from two *Bdnf* mutant embryos revealed no evidence of supernumerary, crest-derived neurons at E14.5 (Fig. 3H).

Table 1
Neuronal number in the facial ganglion of wild-type and *Hoxa2* and *Hoxb1* mutant mice

Genotype	*A2+/+:B1*^{Cre}*+/–*		A2–/–:B1^{Cre}+/–		A2+/+:B1^{Cre}–/–	
	Mean±S.E.	%	Mean±S.E.	%	Mean±S.E	%
Total	991±59 (n=5)	100	3622±253** (n=6)	365	1232±53* (n=6)	124
Placode	933±56 (n=5)	100	828±78^{NS} (n=6)	89	1144±48* (n=6)	122
Crest	58±11 (n=5)	100	2803±228** (n=6)	4832	90±11^{NS} (n=6)	155

Counts of total neurons, neurons that did not express the lineage marker (placode), and neurons that did express the lineage marker (crest) in the facial ganglia of E14.5 embryos. %, percent of *A2+/+; B1*^{Cre}*+/–* value; n, number of ganglia counted; NS: no significant difference from *A2+/+; B1*^{Cre}*+/–* by unpaired Student's t-test; *, $0.01<p<0.05$; **, $p<0.0001$.

Supernumerary, crest-derived neurons express TrkA receptors

The survival of cranial sensory neurons requires the activities of neurotrophins and Trk receptors (Huang and Reichardt, 2001; Huang and Reichardt, 2003). Most facial ganglion neurons require either BDNF or NT3 for survival (Liu and Jaenisch, 2000), and express either TrkB or TrkC, while a small number express TrkA (Matsumoto et al., 2001). When the facial ganglia of *Hoxa2* mutant embryos were examined by immunohistochemistry at E12.5 and E14.5, the crest-derived neurons were found to express TrkA, whereas few neurons in the distal ganglion of mutant embryos or the entire facial ganglion of wild-type embryos expressed this receptor (Figs. 4C, D). TrkA positive processes were observed to extend distally into the facial nerve and proximally into the CNS in the mutants. Whether these TrkA-positive processes establish functional connections was not determined.

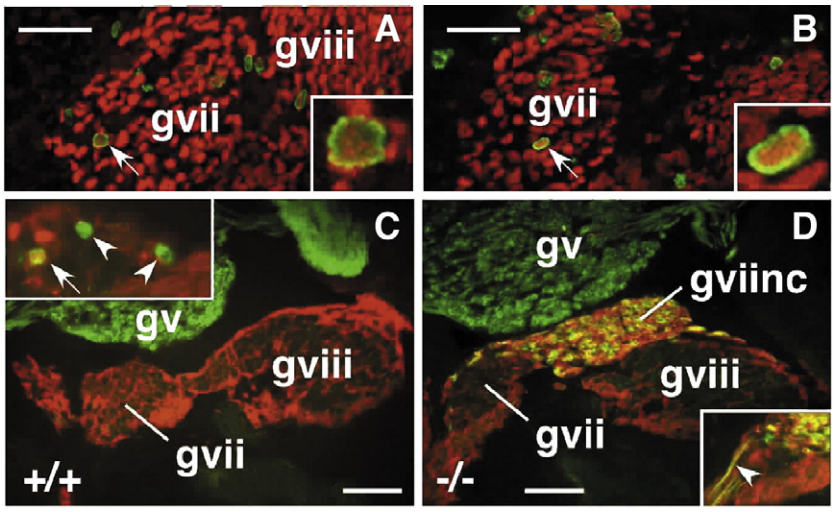

Fig. 4. Neuronal proliferation and TrkA expression in facial ganglia. (A, B) Facial (gvii) and vestibuloacoustic (gviii) ganglia of E10.5 wild-type (A) and *Hoxa2* mutant (B) embryos labeled with antibodies to Islet1/2 (red) to label neurons and phosphohistone H3 (green) to label dividing cells. Arrows indicate doubly labeled cells shown in insets. (C, D) Trigeminal (gv), facial, and vestibuloacoustic ganglia of wild-type (C) and mutant (D) E14.5 embryos labeled with antibodies to the lineage marker (red) and TrkA (green). The facial ganglia of wild-type embryos contained few TrkA-positive neurons, while the trigeminal ganglia contained many. Inset in panel C shows a section of the facial ganglion from another embryo that contains two placode-derived neurons (arrowheads) and one crest-derived neuron (arrow) that expressed TrkA. Most neurons of the crest-derived portion of the facial ganglion in mutant embryos expressed TrkA (D) and TrkA-positive axons exited the ganglion (arrowhead, inset). Scale bars: 50 μm.

Hoxb1 gene dosage does not alter facial ganglion lineages

In principle, a reduction of *Hoxb1* expression caused by the $B1^{Cre}$ null allele could have altered ganglionic lineages in control and *Hoxa2* mutant embryos. Two lines of data suggested this was not the case. Examination of TrkA expression in *Hoxa2* mutant embryos that were wild-type at the *Hoxb1* locus showed that at both E12.5 and E14.5 the same supernumerary population of TrkA-expressing neurons was present (not shown). We also determined the numbers and distributions of labeled and unlabeled neurons in embryos that were homozygous for the $B1^{Cre}$ allele and wild-type at the *Hoxa2* locus. As in $+/B1^{cre}$ embryos, $B1^{Cre}/B1^{Cre}$ embryos showed uniform labeling of the r4-derived neural crest population (Fig. 1E and data not shown). At E14.5, the numbers of crest-derived neurons in $+/B1^{Cre}$ and $B1^{Cre}/B1^{Cre}$ embryos were similar, and the number of unlabeled, placode-derived neurons was, if anything, slightly increased in $B1^{Cre}/B1^{Cre}$ embryos (Table 1). It is therefore unlikely that haploinsufficiency for *Hoxb1* function contributed to the phenotype we have ascribed to the loss of *Hoxa2* function.

Expression of Hoxa2 in the facial ganglion and surrounding tissues

To determine the potential sites of *Hoxa2* gene action, we examined its expression at E9.5 and at E11.5. At E9.5, *Hoxa2* was expressed in the hindbrain, the facial nerve root, and in second branchial arch mesenchyme, but not in the central, neuron-rich portions of the facial and vestibuloacoustic ganglia (Fig. 5A). A layer of non-neuronal cells surrounding the ganglion expressed *Hoxa2*; those surrounding the vestibuloacoustic ganglion did not. We found no evidence of *Hoxa2* expression in the ectodermal placode of the second branchial arch (not shown). Expression was observed in the posterior ectoderm of the arch, as has been reported for the chick (Couly et al., 1998). By E11.5, after many crest-derived neurons were generated in *Hoxa2* mutants, expression in the nerve root and in cells surrounding the facial ganglion had diminished (Fig. 5B). Expression increased in the second arch mesenchyme, and low levels were detected in third arch mesenchyme. Thus, the placode-derived neurons of the facial ganglion, their ectodermal precursors, and the mesenchyme surrounding the facial nerve root and ganglion, did not express detectable levels of *Hoxa2* mRNA from E9.5 to E11.5.

Ectopic gene activation in Hoxa2 mutant embryos

Because the generation of placode- and crest-derived neurons in cranial ganglia is governed by multiple molecular pathways, we sought to determine if some of these were altered by loss of *Hoxa2* function. Neurog1 and Neurog2 are basic helix–loop–helix proteins required for the development of different populations of placode- and crest-derived neurons (Fode et al., 1998; Ma et al., 1998, 1999). *Neurog2* is required for the generation of placode-derived facial ganglion neurons (Fode et al., 1998). We found that *Neurog2* was expressed by the second arch placode of *Hoxa2* mutant embryos at levels comparable to controls (Figs. 5C, D). *Neurog1* is not required for the generation of most facial ganglion neurons, but is essential for the generation of many neural crest-derived neuronal populations (Ma et al., 1998, 1999). *Neurog1* expression could not be detected in the facial ganglia of E11.5 control embryos (Fig. 5E). By contrast, *Neurog1* was strongly expressed in the anterodorsal region of the facial ganglia of *Hoxa2* mutant embryos (Fig. 5F) surrounding and proximal to neuronal cell bodies (Fig. 5G). This corresponds to the position of marker-expressing

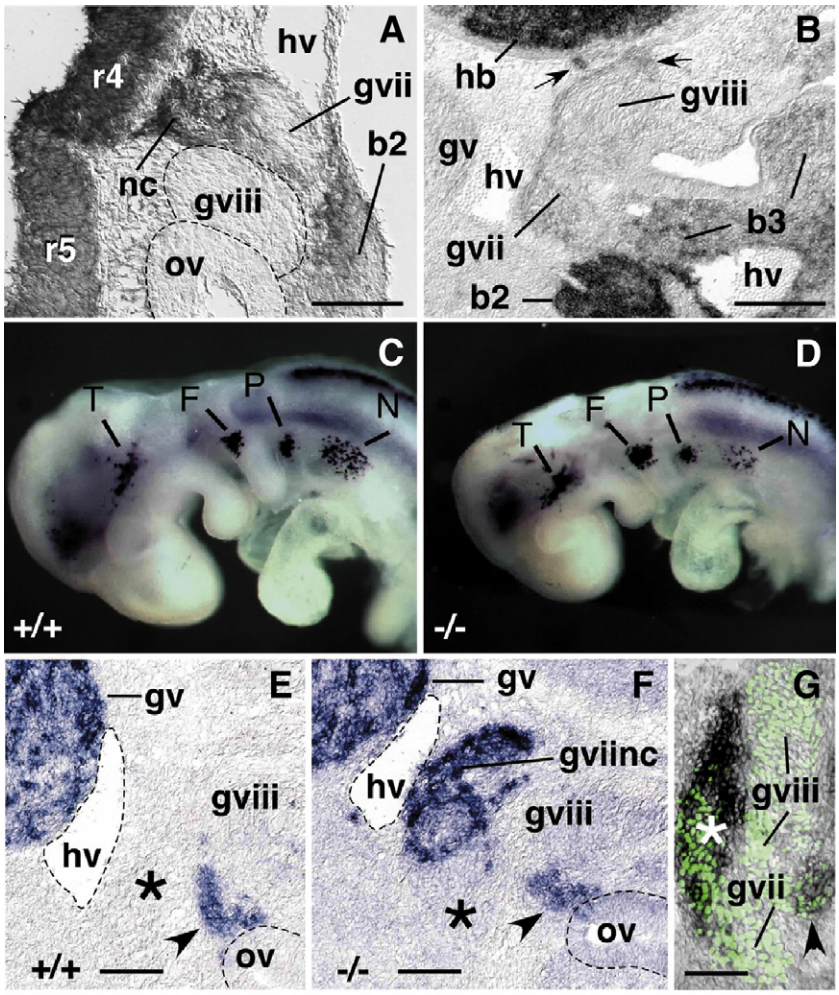

Fig. 5. Expression of molecular markers in wild-type and *Hoxa2* mutant embryos. (A) Horizontal section (anterior to the top and midline to the left) of an E9.5 wild-type embryo labeled with a *Hoxa2* probe. Strong expression was seen in hindbrain rhombomeres 4 and 5 (r4, r5), in the neural crest of the seventh cranial nerve root (nc), and weaker expression was seen in the mesenchyme of the second branchial arch (b2). Expression was not observed in the facial ganglion (gvii). (hv, head vein; gviii, vestibuloacoustic ganglion; ov, otic vesicle). (B) Sagittal section (anterior to the left and dorsal to the top) of an E11.5 embryo. The hindbrain (hb) and mesenchyme of the second branchial arch expressed high levels of *Hoxa2*, and low level expression was seen in rootlets of the seventh and eighth nerves (arrows) and in the mesenchyme of the third branchial arch (b3). Expression in the seventh and eighth ganglia was similar to the background signal observed in the trigeminal ganglion (gv). (C, D) *Neurog2* expression in E9.5 wild-type (C) and *Hoxa2* mutant (D) embryos. The placode for the facial ganglion (F) of the mutant embryo showed apparently normal levels of expression (T, P, N; trigeminal, petrosal, nodose placodes). (E–G) *Neurog1* expression in sagittal sections of E11.5 wild-type (E) and mutant (F, G) embryos. Expression was not seen in the region of the facial ganglion (*, E) in the wild-type embryo, but was seen in cells of the trigeminal ganglion (gv) and in neurons migrating from the otic vesicle (arrowheads) of both. In the mutant embryo, high levels of *Neurog1* were seen in the anterodorsal region of the facial ganglion (*, F). In panel G, Islet1/2 colabeling (green) shows that some of the cells in the region of high Neurog1 expression (*) were neurons. Scale bars: A, B, E, F, 100 μm; G, 50 μm.

neurons at E11.5 (Fig. 3F) and marker- and TrkA-expressing neurons at E12.5 (Fig. 4D and data not shown). Thus, the expression of *Neurog1*, an early component of a neurogenic molecular cascade, was inappropriately activated in the facial ganglia of *Hoxa2* mutants.

Members of the Notch/Delta family of receptors and ligands may regulate neurogenesis and gliogenesis in developing sensory ganglia (Lindsell et al., 1996; Myat et al., 1996; Wakamatsu et al., 2000), although their roles in controlling neurogenesis in cranial ganglia are not established. We were unable to detect *Dll1* transcripts in the facial ganglia of wild-type embryos at E11.5 (Fig. 6A), and *Notch1* expression was marginally higher than background in the central portion of the facial ganglia and elevated at its periphery (Fig. 6C). By contrast, the expression of *Dll1* and *Notch1* was markedly elevated in the facial ganglia of E11.5 *Hoxa2* mutant embryos (Figs. 6B, D). The highest expression for both genes surrounded the more proximal portions of the ganglion (Fig. 6E and data not shown). The expression of *Notch1*, *Dll1*, and *Neurog1* in the facial ganglia of mutant embryos was thus clearly different from that observed in controls, and more closely resembled the expression pattern observed in the trigeminal ganglia of control embryos.

Hoxa2, Pbx1, and Meis1 collectively inhibited spontaneous neuronal differentiation of P19 cells

To test the idea that Hox gene function influences neurogenesis by cell populations capable of adopting both neural and non-neural phenotypes, we overexpressed combinations of Hox proteins and Pbx and Meis transcriptional cofactors in high

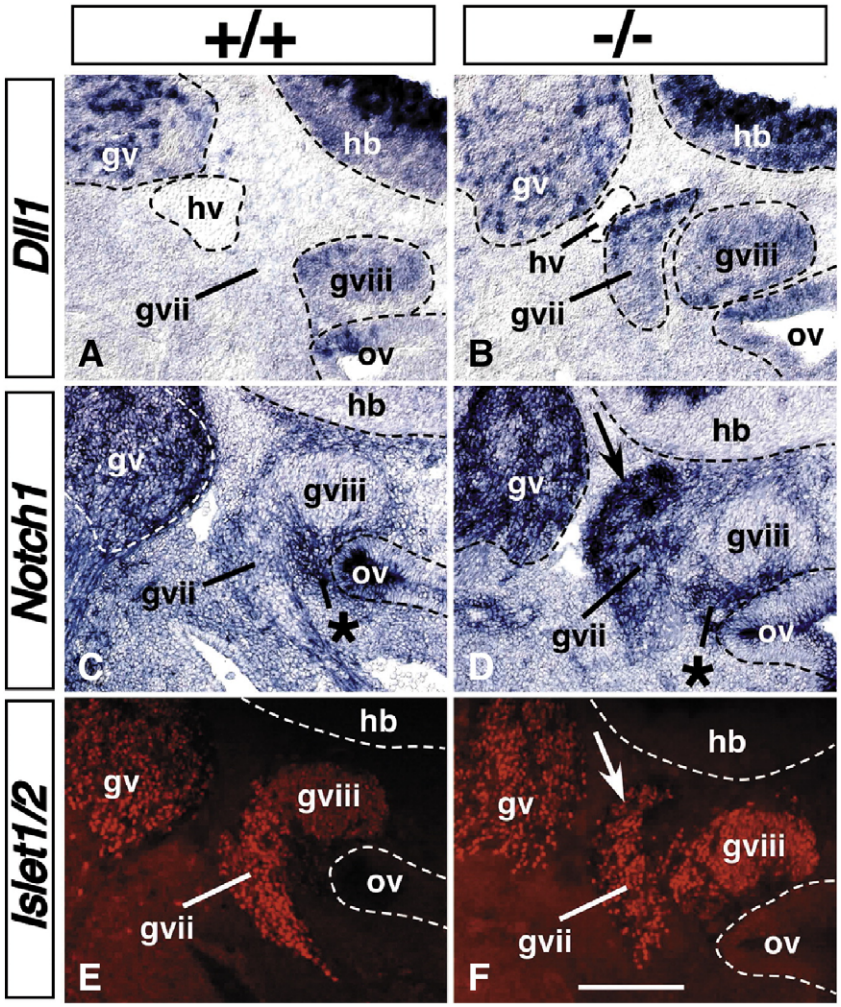

Fig. 6. *Notch1* and *Dll1* expression in wild-type and *Hoxa2* mutant embryos. (A–F) Sagittal sections through the facial ganglia of E11.5 wild-type (A, C, E) and mutant (B, D, F) embryos labeled with probes for *Dll1* (A, B) and *Notch1* (C, D). Panels E and F show the distribution of Islet 1/2 immunoreactivity in the sections shown in panels C and D. Anterior is to the left and dorsal is up in all panels. *Dll1* expression was not observed in the facial ganglia (gvii) of wild-type embryos, and *Notch1* expression was observed only at the periphery of the ganglion, but the expression of both was elevated in the facial ganglia of mutant embryos. Overlap of *Notch1* and Islet1/2 expression in anterodorsal portion of the facial ganglion in the mutant is indicated by arrows in panels D and F. The asterisks in panels C and D indicate expression in cells migrating from the otic vesicle to the vestibuloacoustic ganglion. gv, trigeminal ganglion; gvii, facial ganglion; gviii, vestibuloacoustic ganglion; hb, hindbrain; ov, otic vesicle. Scale bar: F, 200 μm for all panels.

density cultures of P19 cells. P19 embryonal carcinoma cells form a variety of differentiated cell types, and neurogenesis is efficiently induced by aggregation culture in the presence of retinoic acid (Jones-Villeneuve et al., 1982). Low levels of neurogenesis are also seen in the absence of exogenous retinoic acid in long-term cultures or culture under serum-free conditions (Rudniki and McBurney, 1987). Because retinoic acid exposure induces Hox gene expression in embryonal carcinoma cell lines (Featherstone et al., 1988; Popperl and Featherstone, 1993; Simeone et al., 1990) and the expression of Pbx and Meis proteins in P19 cells (Knoepfler and Kamps, 1997), we examined the effect of transfected Hoxa2, Pbx1, and Meis1 on neuronal differentiation in high-density cultures of P19 cells maintained in low-serum medium.

Under the conditions used, transfection efficiencies were uniformly high (ca. 50%) and the frequency of neuronal differentiation was quite low (<5%) (Figs. 7A–C). We therefore determined the fraction of PGP9.5-positive neurons (Wilkinson et al., 1989) that arose from GFP-positive, transfected cells. We found that when cells were transfected with GFP alone, approximately 44% of the neurons arose from transfected cells (Fig. 7D). In cultures simultaneously transfected with *Hoxa2*, *Pbx1*, and *Meis1*, there was a consistent reduction in the number of neurons that arose from transfected cells, to approximately 32% ($p<0.05$, unpaired *t*-test). The frequency of neurogenesis in cultures transfected with *Hoxa2* by itself, or with *Hoxa2* and either *Pbx1* or *Meis1*, was similar to that observed in the GFP control transfections (Fig. 7D and data not shown).

To ask whether the combined activity of Hoxa2 and Pbx1 in these experiments required direct interactions between the proteins, we used a mutation of Hoxa2 that prevents heterodimer formation. Wild-type Hoxa2 contains a pentapeptide sequence (consensus Y/F P W M K/R) amino-terminal to the homeodomain that is required for cooperative DNA binding by Hox and Pbx protein dimers (Knoepfler and Kamps, 1995), and changing the tryptophan residue of this sequence prevents the

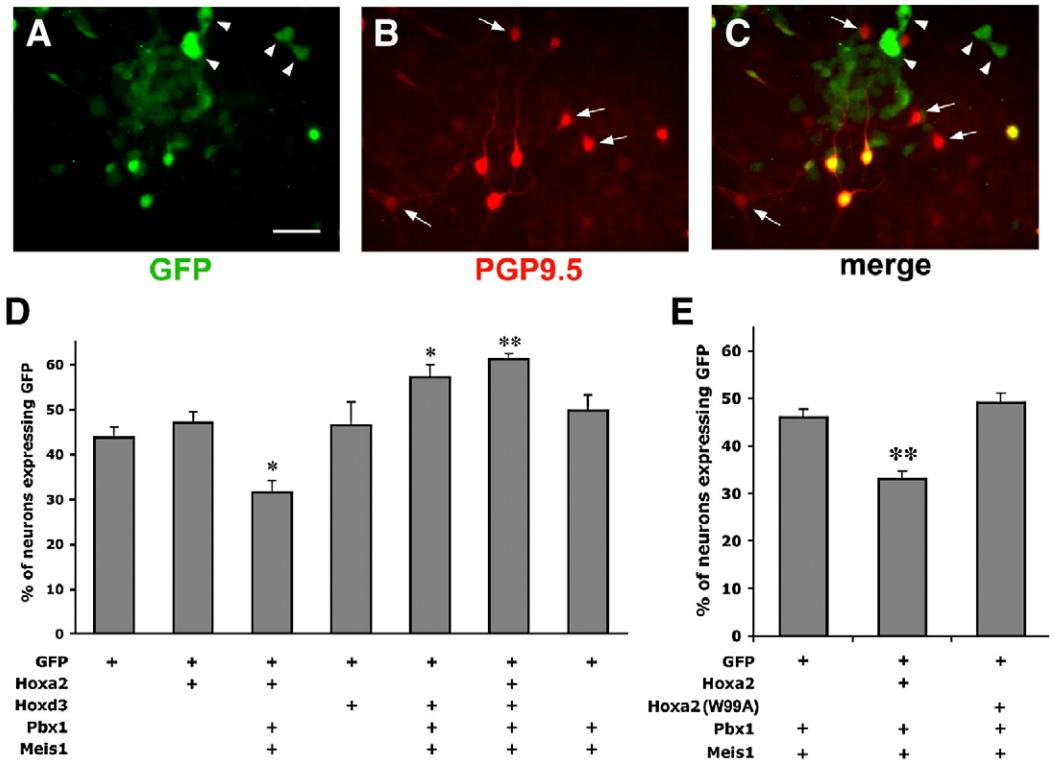

Fig. 7. Neuronal differentiation of P19 cells overexpressing Hox and cofactor proteins 4 days after transfection. (A–C) Immunofluorescence micrographs of a single field showing (A) all transfected cells (GFP, green), (B) cells that have differentiated as neurons (PGP9.5, red), and (C) a merged image. Yellow cells in panel C are transfected cells that differentiated as neurons. Arrowheads in panels A and C indicate transfected cells that did not become neurons, and arrows in panels B and C indicate neurons that differentiated from untransfected cells. Scale bar in panel A indicates 50 μm for panels A–C. (D) Quantification of three independent experiments showing the percentage of neurons (PGP9.5 positive cells) derived from cells transfected with expression plasmids for different combinations of Hox and Hox cofactor proteins (*$p<0.05$ compared to GFP alone, **$p<0.01$ compared to GFP alone or Hoxa2/Pbx1/Meis1). (E) Quantification of three separate experiments using wild-type or mutant Hoxa2 (W99A) (**$p<0.01$ compared to control or Hoxa2 (W99A) transfection).

formation of functional dimers (Neuteboom et al., 1995). We therefore prepared a mutant Hoxa2 expression construct encoding a W99A mutation of the pentapeptide and performed a second set of assays in P19 cells. Cotransfection of the W99A *Hoxa2* mutant together with *Pbx1* and *Meis1* did not alter the base-line level of neuronal differentiation observed in control, GFP-only transfections (Fig. 7E).

We also sought to determine if the inhibition of neurogenesis represented a cell autonomous activity of Hoxa2, or if its expression by surrounding cells could inhibit neurogenesis. We therefore prepared a "test" population of GFP-expressing P19 cells and seeded them at low densities on high density "feeder" layers of P19 cells that had been cotransfected with expression plasmids for *Hoxa2* and the cofactors, or with a control plasmid. There was no difference in the frequency of neuronal differentiation of test cells seeded on either type of feeder layer (Supplementary Fig. 1). This result suggests that the *Hoxa2*-mediated inhibition of neurogenesis we observed represented a cell autonomous activity of *Hoxa2*.

Because we observed ectopic *Neurog1* expression in the facial ganglia of *Hoxa2* mutant embryos (Figs. 5E–G), we attempted to determine if Hoxa2 expression could alter neurogenesis caused by the forced expression of Neurog1 in P19 cells. As reported by others [Farah, 2000 #2316], we found that a high proportion (89%) of P19 cells transfected with a Us2-Neurog1 expression vector differentiated as neurons (Supplementary Fig. 2). This frequency was not altered by simultaneous expression of Hoxa2, Pbx1, and Meis1.Thus, while the analysis of *Hoxa2* mutant mouse embryos suggests that Hoxa2 may repress, directly or indirectly, the expression of Neurog1 from the endogenous locus in vivo, these experiments suggest that the neurogenesis initiated by high levels of Neurog1 is not affected by *Hoxa2*.

Hoxd3 cotransfection relieved Hoxa2-mediated inhibition of neuronal differentiation

These data suggest that *Hoxa2* can repress neurogenesis in pluripotent cell populations, but they also raise the question of how the neural crest cells that arise from rhombomere 6, that also express *Hoxa2*, are able to form neurons of the proximal (superior) ganglion of the ninth cranial nerve. One difference between r4- and r6-derived neural crest cells is that r6-derived cells also express Hox3 paralogues (Manley and Capecchi, 1997), while r4-derived cells do not. To test the possibility that Hox3 paralogues relieve the inhibition of neurogenesis caused by *Hoxa2*, we examined neuronal differentiation in P19 cells cotransfected with *Hoxa2* and *Hoxd3*. In the presence of Pbx and Meis, significantly higher rates of neurogenesis were observed in cultures cotransfected with *Hoxa2* and *Hoxd3* relative

to cultures transfected with *Hoxa2* alone ($p<0.01$, Fig. 7D). Transfection of *Hoxd3* and the cofactors, without *Hoxa2*, also resulted in a consistent elevation of neurogenesis over that seen in GFP control transfection ($p<0.05$), and this increase required the cofactors. These results suggest that Hox3 paralogues antagonize the inhibition of neurogenesis caused by *Hoxa2* in a manner consistent with the principle of posterior prevalence in Hox gene function (Gonzalez-Reyes and Morata, 1990).

Hoxa2-mediated inhibition of neurogenesis in vivo

To determine if the inhibition of neurogenesis observed in transfected P19 cells was relevant to the differentiation of neural crest cells within intact embryos, we used electroporation in chick embryos to force the expression of various combinations of Hoxa2, Pbx1, and Meis1 in neural crest precursors that normally generate both neurons and glia in the trigeminal ganglion. Neural crest cells that migrate to the trigeminal ganglion are derived from the midbrain and r1 and r2 of the hindbrain, and do not express any Hox gene. Although Hoxa2 is expressed within the r2 neural tube, its expression is extinguished in the neural crest cells that emerge from r2 [Prince and Lumsden, 1994 #1285]. We electroporated mixtures of plasmids encoding GFP and Hoxa2, with or without the Pbx1 and Meis1. The electroporations were targeted to the midbrain–hindbrain junction of HH stage 10 embryos (Hamburger Hamilton, 1952), just before the late-migrating NCCs that contribute to the trigeminal ganglia emerge from the neural tube. This avoided significant levels of plasmid expression in the crest-derived ectomesenchyme of the first branchial arch, as occurs after slightly earlier electroporations (Creuzet et al., 2002), and did not generate notable alterations in the organization of craniofacial tissues at the time of harvest (stages 27–28).

In control embryos electroporated with a GFP expression plasmid, approximately 70% of the GFP-expressing cells in the trigeminal ganglia also expressed Islet1/2, identifying them as neurons (Fig. 8). By contrast, when Hoxa2 and both the Pbx1, and Meis1 cofactors were expressed simultaneously, the frequency of neuron differentiation was significantly reduced, to approximately 40% ($p<0.01$). The frequency of neuronal differentiation in a second set of control embryos, electroporated with a plasmid mix that contained Hoxa2 and Pbx1 expression vectors, but omitted the Meis1 vector, did not differ from the GFP-only controls. Thus, the forced expression of

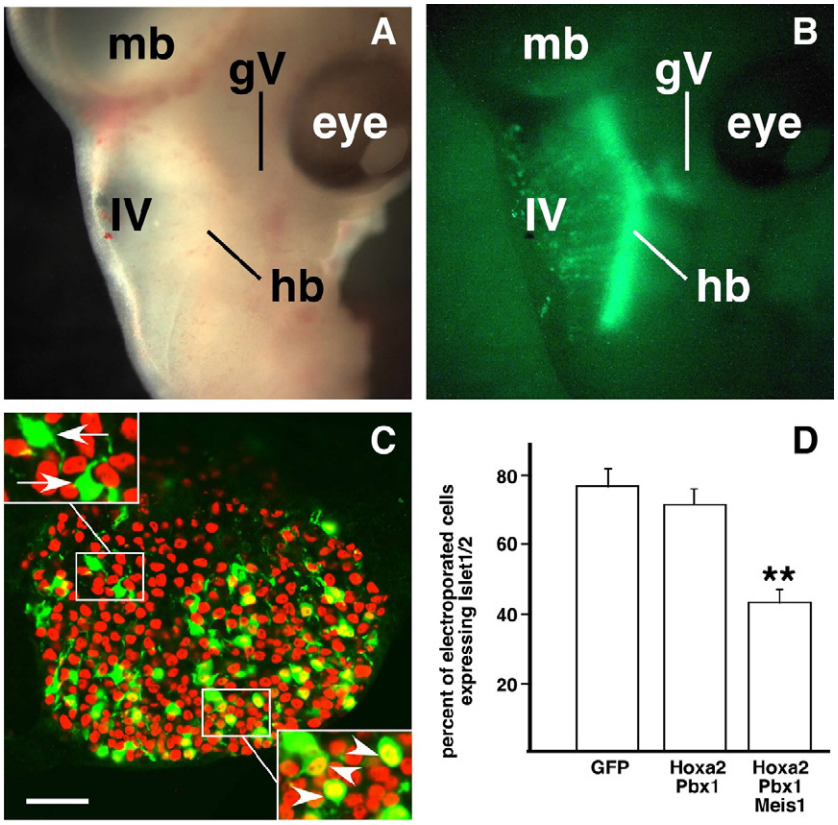

Fig. 8. Neuronal differentiation of neural crest cells in the trigeminal ganglia after in vivo electroporation. (A, B) Lateral views of an electroporated embryo (rostral at top, dorsal at left) under conventional (A) or fluorescence (B) illumination. In panel B, GFP expression is visible in the in the hindbrain (hb) adjacent to the fourth ventrical (VI) and in the trigeminal ganglion (gV). (mb: midbrain). (C) Coronal section through the trigeminal ganglion of a stage 27 embryo that was electroporated at stage 10 with expression plasmids for GFP, Hoxa2, Pbx1, and Meis1, that was stained with antibodies to GFP (green) and Islet 1/2 (red). The inset at lower right shows three GFP-positive neurons with Islet1/2-positive nuclei (arrowheads); the inset at upper left shows two cells whose nuclei did not express Islet1/2 (arrows). (D) Quantification of neuronal differentiation showing the percentage of GFP-positive cell bodies that contained Islet1/2-positive nuclei after electroporation with the indicated expression plasmids. GFP-positive cells in the trigeminal ganglia of embryos transfected with Hoxa2/Pbx1/Meis1 were less likely to differentiate as neurons than those in embryos electroporated with either GFP alone or with Hox2/PBX1 (**$p<0.01$).

exogenous Hoxa2, in the presence of both Pbx1 and Meis1, reduces the frequency of neuronal differentiation by precursors of the trigeminal ganglion.

Discussion

Control of peripheral neurogenesis by Hoxa2

A combination of lineage analyses of *Hoxa2* mutant mouse embryos, overexpression experiments in P19 cells, and misexpression studies in chick embryos has shown that the activity of Hox genes can influence neurogenesis by cranial neural crest cells and pluripotent embryonal carcinoma cells. We found that the facial ganglia of *Hoxa2* mutant embryos contained a population of neurons derived from neural crest cells that was not present in wild-type embryos. The generation of these neurons occurred despite the presence of a grossly normal population of placode-derived neurons. The phenotype suggests that *Hoxa2* expression in r4-derived neural crest cells normally inhibits their ability to differentiate into sensory neurons, and that this inhibition is relieved in the mutants. Additional data consistent with this hypothesis were obtained in transfections of P19 cells, in which *Hoxa2* overexpression caused a reduction in neuronal differentiation, and in experiments in which forcing the expression of Hoxa2 in cells that populate the trigeminal ganglion reduced the probability of neuronal differentiation. In both P19 cells and chick embryos, the reduction of neurogenesis required the presence of Pbx and Meis cofactors. In P19 cells, Hoxa2-mediated inhibition of neurogenesis was abolished by mutation of the Hox protein domain required for dimerization of Hox and Pbx proteins, and could be antagonized by a member of the Hox3 paralogous group.

In mouse embryos, the absence of *Hoxa2* expression clearly affected the generation of facial ganglion sensory neurons by r4-derived neural crest cells, but did not appear to alter the generation of parasympathetic neurons of the ptergopalatine ganglion by the same crest population. The signaling cascades that control sensory and parasympathetic neuron differentiation are distinct from one another. The apparently normal generation of r4-derived parasympathetic neurons in the ptergopalatine ganglion suggests that *Hoxa2* does not influence the signaling pathways, including *Mash1* and *Phox2a* among other factors, that regulate parasympathetic neurogenesis (Hirsch et al., 1998; Lo et al., 1998; Morin et al., 1997). By contrast, the appearance of crest-derived sensory neurons in the facial ganglia of the mutants was accompanied by a striking upregulation of *Neurog1* expression, and increases in *Notch1* and *Dl1* expression as well. *Neurog1* is required for the generation of sensory neurons by cranial neural crest cells (Ma et al., 1999), and in a number of systems, *Neurog1* overexpression, by itself, is sufficient to induce ectopic neurogenesis (Ma et al., 1996). In transfections of P19 cells, we found that *Hoxa2* expression could not antagonize neurogenesis promoted by forced *Neurog1* overexpression. This result does not address the question of whether Hoxa2 normally represses, directly or indirectly, the expression of the endogenous mouse *Neurog1* locus in vivo. It does, however, suggest that Hoxa2 cannot significantly inhibit neurogenic mechanisms that are initiated by Neurog1 expression. Our results are most consistent with the idea that *Hoxa2* acts upstream of *Neurog1* in neural crest cells to inhibit neurogenesis, and that the mutant phenotype reflects a loss of this inhibition.

The generation of neurons by r4-derived neural crest cells in *Hoxa2* mutant embryos is unlikely to substantially alter the generation of glial cells by the same lineage. Cranial neural crest cell populations are capable of remarkable levels of regulative migration, proliferation, and differentiation, including the complete reconstitution of neuronal and glial populations of cranial ganglia following surgical manipulations (Couly et al., 1996). Additionally, the survival and proliferation of glial cell precursors are regulated by factors in the local environment, including many that are produced by differentiating neurons (Anderson, 1997; Dong et al., 1995; Wakamatsu et al., 2000). We therefore speculate that the generation of crest-derived neurons in the proximal portion of the facial ganglion of *Hoxa2* mutant embryos is likely to result in a local increase in the survival and/or proliferation of glial precursors within the same r4-derived neural crest cell population. We think it is unlikely that the generation of these neurons has any effect on the proliferation or differentiation of the ectomesenchymal derivatives of the r4 neural crest, which have migrated beyond the ganglionic anlagen by the time the supernumerary crest-derived neurons begin to differentiate.

Fidelity of lineage marking by the $B1^{Cre}$ allele

The labeling of peripheral neurons and glia by the combination of the $B1^{Cre}$ and *R26R* alleles appeared to be virtually complete and highly selective. Neural crest cells populate the branchial arches in a distal to proximal order (Serbedzija et al., 1992), so the first cells to emerge from the hindbrain form distal ectomesenchyme. Although there is only a narrow temporal window between the onset of *Hoxb1* expression (Frohman et al., 1990) and the generation of neural crest (Nichols, 1986; Serbedzija et al., 1992), we found that the most distal ectomesenchyme in the second arch was labeled, indicating that the marker was recombined in the earliest neural crest cells to migrate out of r4. Cell populations known to arise from non-crest lineages were not labeled, including the ectoderm, the mesodermal core, and the vascular endothelium (Le Douarin, 1983). In addition to r4-derived neural crest, the second branchial arch is thought to contain small contributions from r3- and r5-derived crest (Lumsden et al., 1991; Sechrist et al., 1993; Serbedzija et al., 1992). We did not observe recombination in r3, and only low levels of recombination in r5, and yet we were unable to find more than a rare unlabeled ectomesenchymal cell in the second arch. We did observe a small population of unmarked glial cells in the facial ganglion in wild-type embryos that could have been derived from r3 or r5 neural crest cells. The small number of unlabeled cells in distal portions of the second branchial arch suggests that r3- and r5-derived cells do not proliferate extensively, that they do not survive, or that they are restricted to the margins of the labeled territories, where they would not be recognized as part of the second arch in these preparations.

It is unlikely that the phenotype we observed in *Hoxa2* mutant embryos was caused by the presence of the null, $B1^{Cre}$ allele used to mark the r4-derived lineages. Supernumerary, TrkA-positive neurons were present in the ganglia of *Hoxa2*-mutant embryos that were wild-type at the *Hoxb1* locus (*Hoxa2*−/−:*Hoxb1*+/+), and, conversely, were absent in embryos that lacked all *Hoxb1* function and were wild-type at the *Hoxa2* locus (*Hoxa2*+/+:$Hoxb1^{Cre}/Hoxb1^{Cre}$). It is also unlikely that the phenotype is due to alterations in the expression of adjacent Hoxa family members, similar to the alterations shown for recombinant alleles of some other Hox genes (Aubin et al., 1998; Barrow and Capecchi, 1996; Ren et al., 2002; Rijli et al., 1994), because the expression of *Hoxa1* and *Hoxa3* is reported to be unaltered in *Hoxa2* mutant embryos (Gendron-Maguire et al., 1993; Rijli et al., 1993).

The results reported here differ from those of an earlier report that also described the fates of neural crest cells derived from *Hoxb1*-expressing neuroepithelium (Arenkiel et al., 2003). Both studies agree on the predominantly glial fates of second arch cells in the facial ganglion. Whereas Arenkiel et al. (2003) did not comment on the lineage of the ptergopalatine ganglion in their report, here we found that the neurons of this ganglion arose from second arch neural crest cells. Significantly, this establishes that neither *Hoxb1* nor *Hoxa2* expression in the r4 neuroepithelium or in the neural crest derived from r4, by themselves, preclude neurogenesis. Although both *Hoxa2* and *Hoxb1* are expressed in the r4 neuroepithelium, we (Fig. 1F) and others (Frohman et al., 1990; Murphy et al., 1989) have found that *Hoxb1* expression is extinguished as crest cells emerge from r4, while *Hoxa2* expression is maintained at high levels in the same cells. The generation of facial ganglion neurons by r4-derived crest in *Hoxa2* mutants and the lack of such neurogenesis in *Hoxb1* mutants strongly argue that the inhibition of sensory neuron fates within the facial ganglion during normal embryogenesis is a consequence of *Hoxa2*, and not *Hoxb1*, gene function.

We additionally found that r4-derived glial cells were associated with both motor and sensory components of the facial nerve. Although Arenkiel et al. (2003) did not illustrate the finding, they reported that r4-derived crest associated exclusively with motor components, and did not associate with sensory axons. Here, r4-derived neural crest cells were present in the most distal portions of the chorda tympani, associated with sensory axons that innervate lingual taste buds. r4-derived cells also formed the glia associated with the axons running between the acoustic ganglion and the otic vesicle.

There are several possible explanations for this difference between the reports. Cre may be more efficiently expressed from the fusion allele used here because it would not require re-initiation of translation from a bicistronic message, as would be the case (Gorski and Jones, 1999) for the IRES-Cre cassette used by Arenkiel et al. (2003). We favor this explanation because Arenkiel et al. illustrated incomplete activation of reporter expression in the motor neuron axons and glia of a purely motor branch of the facial nerve, suggesting that marker activation may be incomplete elsewhere as well. Alternatively, it could also be argued that we see labeling of glia associated with sensory axons because the $B1^{Cre}$ allele ectopically activated the reporter in cells that do not normally express *Hoxb1*. Given that the timing and distribution of Cre expression duplicated that of *Hoxb1*, and that reporter expression closely resembled the cumulative pattern of *Hoxb1* expression, we feel this explanation is unlikely. Finally, it is possible that the difference between the sets of findings is due to unrecognized differences in genetic background among the mouse strains used, though we again think this is not likely to be the explanation.

Site of Hoxa2 gene action

The repression of sensory neurogenesis in the facial ganglion of wild-type embryos could result from a cell autonomous activity of *Hoxa2*, or from cell–cell interactions between crest cells in the ganglionic anlagen and those forming the ectomesenchyme of the second arch, which also express *Hoxa2*. Both the pattern of *Hoxa2* expression in wild-type embryos and our P19 cell transfections suggest that the inhibition is mediated by cell autonomous mechanisms. In mutant embryos, neurogenesis by crest cells began between E10.5 and E11.5. In wild-type embryos, the mesenchymal cells expressing high levels of *Hoxa2* mRNA had migrated past the facial ganglion by E9.5, and the mesenchymal cells surrounding the ganglion did not express *Hoxa2* mRNA. In contrast, high levels of *Hoxa2* mRNA were observed in cells within the proximal nerve root, the region where crest-derived neurons first appeared in mutant embryos. Thus, in wild-type embryos, *Hoxa2* was expressed in the population of cells that generated the supernumerary neurons in the mutants, and was not expressed at appreciable levels in surrounding tissues.

The argument that Hoxa2 acts in a cell autonomous manner to repress neurogenesis was strengthened by experiments in which Hoxa2, Pbx1, and Meis1 were over-expressed in P19 cells and first brachial arch neural crest cells in chick embryos. In both cases, the misexpression led to reproducible reductions in the frequency of neuronal differentiation. In P19 cells, the frequency of neuronal differentiation in a test population was not influenced by expression of Hoxa2, Pbx1 and Meis1 in feeder cell layers. In the chick embryo electroporations, the GFP-expressing cells were dispersed throughout the trigeminal ganglia, making it unlikely that the transfected cells expressing Hoxa2 affected one another through cell interactions. Collectively, these experiments suggest that the reduction of neuronal differentiation in P19 cells, the reduction in trigeminal neurogenesis in electroporated chick embryos, and the small number of crest-derived neurons present in the facial ganglia of wild-type embryos are each due to a cell autonomous activity of *Hoxa2*.

The transfection data also add to accumulating evidence (Knoepfler and Kamps, 1997) that the Pbx and Meis proteins, probably through their interactions with Hox proteins, are key players in the control of neuronal differentiation in P19 cells (Knoepfler and Kamps, 1997; Qin et al., 2004a,b). It has long been recognized that the induction of neuronal differentiation by retinoic acid in embryonal carcinoma cells, including P19 cells, is associated with increased expression of multiple *Hox*

genes (Pratt et al., 1993). More recently, it has been found that retinoic acid also leads to increases in the levels of Pbx and Meis proteins (Knoepfler and Kamps, 1997; Qin et al., 2004a), and that reducing Pbx protein levels, through the use of antisense or short interfering RNA's, reduces neuronal differentiation in retinoic acid treated P19 cells (Qin et al., 2004b).

Pbx and Meis proteins are TALE (three amino acid loop extension) homeodomain transcription factors that modulate the activity of many members of the *Hox* gene family (Moens and Selleri, 2006). The association of Hox and Pbx proteins in DNA-bound complexes requires a pentapeptide sequence (F/YPWMR/K) amino-terminal to the homeodomain of the Hox partner (Knoepfler et al., 1999). The cooperative binding of Hox and Pbx proteins alters the binding affinity and specificity of the Hox partner, and typically increases transcription of target genes, although more complex interactions that depend on cellular context have also been reported (Saleh et al., 2000). We are not aware of prior reports describing alterations in the frequency of neuronal differentiation of P19 cells that are caused by misexpression of Hox family members. Here, we found that P19 cells overexpressing Hoxa2 or Hoxd3 exhibited reproducible changes in the frequency of neurogenesis, that these changes were only observed in the presence of the Pbx and Meis cofactors, and that the Hoxa2-mediated inhibition was not observed when the critical tryptophan residue of the peptide (F/YPWMR/K) required for interaction with Pbx proteins (Knoepfler and Kamps, 1995) was mutated.

Hox genes and peripheral neurogenesis

We suggest that phenotype of the facial ganglion in *Hoxa2* mutant embryos represents an anterior transformation of the developmental potential of a set of cranial neural crest cells, similar to that seen in mesenchymal tissues of *Hoxa2* mutants (Gendron-Maguire et al., 1993; Rijli et al., 1993), and in a variety of skeletal and CNS tissues of animals lacking various single Hox gene functions (Duboule and Morata, 1994; Gonzalez-Reyes et al., 1990). The transformation appears to be limited to the generation of ectopic neurons, and does not extend to the formation of connections between these neurons and the targets normally innervated by trigeminal ganglion neurons (data not shown). Differences in the terminal fates of neural crest cells generated at different levels of the body axis, and in particular the differentiation of sensory and autonomic neurons, are strongly influenced by the tissues through which crest cells migrate and in which they settle (Baker et al., 1997; Le Douarin and Smith, 1988). This applies to the generation of neuronal and non-neuronal cells by cranial neural crest cells as well. For example, the normally gliogenic crest cells of the nodose ganglion form neurons when they are transplanted to the trunk (Ayer-LeLievre and LeDouarin, 1982). Additionally, the removal of placode-derived neurons through surgical ablation (Harrison et al., 1995) or by genetic means (Fode et al., 1998) can induce neural crest cells that normally do not form neurons to generate large numbers of neurons.

An exception to the dominant role of surrounding tissues in the determination of neural crest cell fates is the control of ectomesenchymal fates of first and second branchial arch neural crest cells by Hox gene function. Transplantation of the Hox-negative frontonasal, mesencephalic, or metencephalic neural folds into more posterior levels results in the ectopic formation of bones of the lower jaw (Noden, 1983), which likely results from the repression of Hoxa2 expression by FGF8 signaling from the transplanted tissue (Trainor et al., 2002). Conversely, *Hox*-expressing neural crest cells from the hindbrain do not form appropriate facial skeletal elements when transplanted into the first branchial arch domain (Couly et al., 1998), and the misexpression of Hox genes in first branchial arch neural crest cells also prevents the formation of facial skeletal structures normally derived from these cells (Creuzet et al., 2002).

In these paradigms, a key feature of the transposed crest cell populations is the presence or absence of the expression of any of several Hox genes. By contrast, the repression of neurogenesis reported here is likely to be specific to *Hoxa2*, as Hox genes are expressed in other cranial crest cell populations that do generate neurons. The idea that Hoxa2 function represses neurogenesis may explain phenotypic attributes of embryos with reduced Hox3 paralogous group function. In embryos lacking function of any two *Hox3* group genes, neurons of the proximal portion of the ninth cranial ganglion, normally derived from neural crest cells that arise from the posterior hindbrain, are often missing (Manley and Capecchi, 1997). As both *Hoxa2* and members of the Hox3 paralogous group are expressed in these neural crest cells, it is possible that, in the absence of sufficient *Hox3* function, the normally inapparent inhibition of neurogenesis by *Hoxa2* becomes apparent. Our observation that the inhibition of neurogenesis by *Hoxa2* was antagonized by the simultaneous expression of *Hoxd3* in P19 cell cultures is consistent with this mechanism. Both the mutant phenotypes and the results of the P19 cell transfections are also consistent with the posterior prevalence of Hox gene functions (Duboule, 1991; Gonzalez-Reyes and Morata, 1990). By this argument, *Hoxa2* activity in second branchial neural crest cells arch suppresses the capacity for neurogenesis shown by the Hox-negative first branchial arch neural crest, and the function of Hox paralogous group 3 gene in the third branchial arch antagonizes this repression of neurogenesis by *Hoxa2*.

Two stages of neurogenesis

Biphasic patterns of neurogenesis occur in sensory ganglia at all levels of the neuraxis. Placode-derived neurons are born before crest-derived neurons in cranial ganglia (Altman and Bayer, 1982; d'Amico-Martel and Noden, 1980). In spinal dorsal root ganglia, *Neurog2*-dependent neurons arise before *Neurog1*-dependent neurons (Ma et al., 1999). Furthermore, the two phases are largely independent of one another. Placode-derived neurons of the seventh, ninth, and tenth ganglia are generated in the absence of *Neurog1* function, as are the *Neurog2*-dependent neurons of spinal dorsal root ganglia (Ma et al., 1998, 1999). Loss of *Neurog2* function leads to a slight delay in the onset of *Neurog1*-dependent neurogenesis in spinal

dorsal root ganglia, but the *Neurog1*-dependent neurons eventually form substantial populations (Ma et al., 1999).

In *Hoxa2* mutant embryos, crest-derived neurons arose after placode-derived neurons had assembled in the ganglionic anlagen. The onset of crest-derived neurogenesis may mark the point at which second brachial arch crest cells become competent to differentiate as neurons. This would be consistent with the timing of neurogenesis, presumably by neural crest, in the facial ganglia of *Neurog2* mutant embryos (Fode et al., 1998). Placode-derived facial ganglion neurons are not generated in these embryos, there are no neurons present at E10.5, but a substantial population is present at E12.5. If the initial failure of crest to generate neurons represents an active repression of neurogenic potential, then the timing of neurogenesis in these two mutants suggests that this early repression is independent of the presence of placode-derived neurons, which are present in the *Hoxa2* mutants, or *Hoxa2* function, which is present in the *Neurog2* mutants. Alternatively, if it represents a delayed acquisition of neurogenic potential, then this potential is normally subject to further inhibition by *Hoxa2*, and this inhibition can be overridden by the absence of placode-derived neurons.

Conclusion

A large body of experimentation has established that neural crest cells are endowed with broad developmental potential (Le Douarin, 1983), that their differentiation is strongly influenced by signals generated by surrounding tissues, and that under appropriate conditions even fates traditionally considered incompatible with one another can be adopted (McGonnell and Graham, 2002). Nonetheless, in the intact embryo, particular subsets of the potential fates are adopted by cohorts of neural crest cells that arise at specific times and at particular axial levels. Although Hox gene expression is a major determinant of axial patterning in the embryo, differences in peripheral neurogenic fates of neural crest cells have not typically been associated with temporal or spatial differences in Hox gene activity. The results presented here suggest that a closer examination of the relationship between Hox gene expression and the neuronal fates of neural crest cells is warranted.

Acknowledgments

We thank Elizabeth Robertson for the CCE embryonic stem cells and instruction in their use, Phillipe Soriano for the *R26R* mice, David Katz for providing the *Bdnf* mutant mice, and Samuel Pfaff for providing the in situ hybridization protocol. We also thank Amy Lucky for technical assistance, Katherine Lobur for help with the mice, Ron Conlon for providing several probes, David Anderson for the Sox10 antibody, and Evan Deneris, Alison Hall, David Katz, Robert Miller, Lynn Landmesser, and Catherine Rottkamp for helpful discussions. The 39.4D5 antibody to Islet proteins, developed by Thomas Jessell, was obtained from the Developmental Studies Hybridoma Bank under the auspices of the NICHD and maintained by the University of Iowa, Department of Biological Studies.

Appendix A. Supplementary data

Supplementary data associated with this article can be found, in the online version, at doi:10.1016/j.ydbio.2007.11.032.

References

Altman, J., Bayer, S.A., 1982. Development of the cranial nerve ganglia and related nuclei in the rat. Adv. Anat. Embryol. Cell Biol. 74, 1–90.
Anderson, D.J., 1997. Cellular and molecular biology of neural crest cell lineage determination. Trends Genet. 13, 276–280.
Arenkiel, B.R., et al., 2003. Hoxb1 neural crest preferentially form glia of the PNS. Dev. Dyn. 227, 379–386.
Aubin, J., et al., 1998. Transcriptional interferences at the Hoxa4/Hoxa5 locus: importance of correct Hoxa5 expression for the proper specification of the axial skeleton. Dev. Dyn. 212, 141–156.
Ayer-LeLievre, C.S., LeDouarin, N.M., 1982. The early development of cranial sensory ganglia and the potentialities of their component cells studied in quail-chick chimeras. Dev. Biol. 94, 291–310.
Baker, C.V., et al., 1997. Early- and late-migrating cranial neural crest cell populations have equivalent developmental potential in vivo. Development 124, 3077–3087.
Barrow, J.R., Capecchi, M.R., 1996. Targeted disruption of the Hoxb-2 locus in mice interferes with expression of Hoxb-1 and Hoxb-4. Development 122, 3817–3828.
Bettenhausen, B., et al., 1995. Transient and restricted expression during mouse embryogenesis of Dll1, a murine gene closely related to *Drosophila* Delta. Development 121, 2407–2418.
Boudreau, N., et al., 1997. Induction of the angiogenic phenotype by Hox D3. J. Cell Biol. 139, 257–264.
Conlon, R.A., et al., 1995. Notch1 is required for the coordinate segmentation of somites. Development 121, 1533–1545.
Conover, J.C., et al., 1995. Neuronal deficits, not involving motor neurons, in mice lacking BDNF and/or NT4. Nature 375, 235–238.
Couly, G., et al., 1996. The regeneration of the cephalic neural crest, a problem revisited: the regenerating cells originate from the contralateral or from the anterior and posterior neural fold. Development 122, 3393–3407.
Couly, G., et al., 1998. Determination of the identity of the derivatives of the cephalic neural crest: incompatibility between Hox gene expression and lower jaw development. Development 125, 3445–3459.
Couly, G., et al., 2002. Interactions between Hox-negative cephalic neural crest cells and the foregut endoderm in patterning the facial skeleton in the vertebrate head. Development 129, 1061–1073.
Creuzet, S., et al., 2002. Negative effect of Hox gene expression on the development of the neural crest-derived facial skeleton. Development 129, 4301–4313.
d'Amico-Martel, A., Noden, D.M., 1980. An autoradiographic analysis of the development of the chick trigeminal ganglion. J. Embryol. Exp. Morphol. 55, 167–182.
d'Amico-Martel, A., Noden, D.M., 1983. Contributions of placodal and neural crest cells to avian cranial peripheral ganglia. J. Comp. Neurol. 166, 445–468.
Davenne, M., et al., 1999. Hoxa2 and Hoxb2 control dorsoventral patterns of neuronal development in the rostral hindbrain. Neuron 22, 677–691.
Dong, Z., et al., 1995. Neu differentiation factor is a neuron-glia signal and regulates survival, proliferation, and maturation of rat Schwann cell precursors. Neuron 15, 585–596.
Duboule, D., 1991. Patterning in the vertebrate limb. Curr. Opin. Genet. Dev. 1, 211–216.
Duboule, D., Morata, G., 1994. Colinearity and functional hierarchy among genes of the homeotic complexes. Trends Genet. 10, 358–364.
Dunwoodie, S.L., et al., 1997. Mouse Dll3: a novel divergent Delta gene which may complement the function of other Delta homologues during early pattern formation in the mouse embryo. Development 124, 3065–3076.
Ericson, J., et al., 1992. Early stages of motor neuron differentiation revealed by expression of homeobox gene Islet-1. Science 256, 1555–1560.
Featherstone, M.S., et al., 1988. Hox-5.1 defines a homeobox-containing gene

locus on mouse chromosome 2. Proc. Natl. Acad. Sci. U. S. A. 85, 4760–4764.
Fode, C., et al., 1998. The bHLH protein Neurogenin 2 is a determination factor for epibranchial placode-derived sensory neurons. Neuron 20, 483–494.
Frohman, M.A., et al., 1990. Isolation of the mouse Hox-2.9 gene; analysis of embryonic expression suggests that positional information along the anterior-posterior axis is specified by mesoderm. Development 110, 589–607.
Gendron-Maguire, M., et al., 1993. Hoxa-2 mutant mice exhibit homeotic transformation of skeletal elements derived from cranial neural crest. Cell 75, 1317–1331.
Goddard, J.M., et al., 1996. Mice with targeted disruption of Hoxb-1 fail to form the motor nucleus of the VIIth nerve. Development 122, 3217–3228.
Gonzalez-Reyes, A., Morata, G., 1990. The developmental effect of over-expressing a Ubx product in *Drosophila* embryos is dependent on its interactions with other homeotic products. Cell 61, 515–522.
Gonzalez-Reyes, A., et al., 1990. Are cross-regulatory interactions between homeotic genes functionally significant. Nature 344, 78–80.
Gorski, J.A., Jones, K.R., 1999. Efficient bicistronic expression of cre in mammalian cells. Nucleic Acids Res. 27, 2059–2061.
Grammatopoulos, G.A., et al., 2000. Homeotic transformation of branchial arch identity after Hoxa2 overexpression. Development 127, 5355–5365.
Harrison, T.A., et al., 1995. Compensatory responses and development of the nodose ganglion following ablation of placodal precursors in the embryonic chick (*Gallus domesticus*). Cell Tissue Res. 281, 379–385.
Hirsch, M.R., et al., 1998. Control of noradrenergic differentiation and Phox2a expression by MASH1 in the central and peripheral nervous system. Development 125, 599–608.
Huang, E.J., Reichardt, L.F., 2001. Neurotrophins: roles in neuronal development and function. Annu. Rev. Neurosci. 24, 677–736.
Huang, E.J., Reichardt, L.F., 2003. TRK receptors: roles in neuronal signal transduction. Annu. Rev. Biochem. 72, 609–642.
Jones, K.R., et al., 1994. Targeted disruption of the BDNF gene perturbs brain and sensory neuron development but not motor neuron development. Cell 76, 989–999.
Jones-Villeneuve, E.M., et al., 1982. Retinoic acid induces embryonal carcinoma cells to differentiate into neurons and glial cells. J. Cell Biol. 94, 253–262.
Knoepfler, P.S., Kamps, M.P., 1995. The pentapeptide motif of Hox proteins is required for cooperative DNA binding with Pbx1, physically contacts Pbx1, and enhances DNA binding by Pbx1. Mol. Cell. Biol. 15, 5811–5819.
Knoepfler, P.S., Kamps, M.P., 1997. The Pbx family of proteins is strongly upregulated by a post-transcriptional mechanism during retinoic acid-induced differentiation of P19 embryonal carcinoma cells. Mech. Dev. 63, 5–14.
Knoepfler, P.S., et al., 1999. A conserved motif N-terminal to the DNA-binding domains of myogenic bHLH transcription factors mediates cooperative DNA binding with pbx-Meis1/Prep1. Nucleic Acids Res. 27, 3752–3761.
Kuhlbrodt, K., et al., 1998. Sox10, a novel transcriptional modulator in glial cells. J. Neurosci. 18, 237–250.
Le Douarin, N., 1983. The Neural Crest. Cambridge Univ. Press, Cambridge.
Le Douarin, N., Smith, J., 1988. Development o the peripheral nervous system from the neural crest. Annu. Rev. Cell Biol. 4, 375–404.
Lee, M.K., et al., 1990. The expression and posttranslational modification of a neuron-specific beta-tubulin isotype during chick embryogenesis. Cell Motil. Cytoskeleton 17, 118–132.
Lindsell, C.E., et al., 1996. Expression patterns of Jagged, Delta1, Notch1, Notch2, and Notch3 genes identify ligand-receptor pairs that may function in neural development. Mol. Cell. Neurosci. 8, 14–27.
Liu, X., Jaenisch, R., 2000. Severe peripheral sensory neuron loss and modest motor neuron reduction in mice with combined deficiency of brain-derived neurotrophic factor, neurotrophin 3 and neurotrophin 4/5. Dev. Dyn. 218, 94–101.
Lo, L., et al., 1998. MASH1 activates expression of the paired homeodomain transcription factor Phox2a, and couples pan-neuronal and subtype-specific components of autonomic neuronal identity. Development 125, 609–620.
Lo, L., et al., 2002. Comparison of the generic neuronal differentiation and neuron subtype specification functions of mammalian achaete-scute and atonal homologs in cultured neural progenitor cells. Development 129, 1553–1567.
Lumsden, A., et al., 1991. Segmental origin and migration of neural crest cells in the hindbrain region of the chick embryo. Development 113, 1281–1291.
Ma, Q., et al., 1996. Identification of neurogenin, a vertebrate neuronal determination gene. Cell 87, 43–52.
Ma, Q., et al., 1998. Neurogenin1 is essential for the determination of neuronal precursors for proximal cranial sensory ganglia. Neuron 20, 469–482.
Ma, Q., et al., 1999. Neurogenin1 and Neurogenin2 control two distinct waves of neurogenesis in developing dorsal root ganglia. Genes Dev. 13, 1717–1728.
Manley, N.R., Capecchi, M.R., 1997. Hox group 3 paralogous genes act synergistically in the formation of somitic and neural crest-derived structures. Dev. Biol. 192, 274–288.
Matsumoto, I., et al., 2001. A comparative study of three cranial sensory ganglia projecting into the oral cavity: in situ hybridization analyses of neurotrophin receptors and thermosensitive cation channels. Brain Res. Mol. Brain Res. 93, 105–112.
McGonnell, I.M., Graham, A., 2002. Trunk neural crest has skeletogenic potential. Curr. Biol. 12, 767–771.
Moens, C.B., Selleri, L., 2006. Hox cofactors in vertebrate development. Dev. Biol. 291, 193–206.
Morin, X., et al., 1997. Defects in sensory and autonomic ganglia and absence of locus coeruleus in mice deficient for the homeobox gene Phox2a. Neuron 18, 411–423.
Murphy, P., Hill, R.E., 1991. Expression of the mouse labial-like homeobox-containing genes, Hox 2.9 and Hox 1.6, during segmentation of the hindbrain. Development 111, 61–74.
Murphy, P., et al., 1989. Segment-specific expression of a homoeobox-containing gene in the mouse hindbrain. Nature 341, 156–159.
Myat, A., et al., 1996. A chick homologue of Serrate and its relationship with Notch and Delta homologues during central neurogenesis. Dev. Biol. 174, 233–247.
Neuteboom, S.T., et al., 1995. The hexapeptide LFPWMR in Hoxb-8 is required for cooperative DNA binding with Pbx1 and Pbx2 proteins. Proc. Natl. Acad. Sci. U. S. A. 92, 9166–9170.
Nichols, D.H., 1986. Formation and distribution of neural crest mesenchyme to the first pharyngeal arch region of the mouse embryo. Am. J. Anat. 176, 221–231.
Noden, D.M., 1983. The role of the neural crest in patterning of avian cranial skeletal, connective, and muscle tissues. Dev. Biol. 96, 144–165.
O'Gorman, S., et al., 1991. Recombinase-mediated gene activation and site-specific integration in mammalian cells. Science 251, 1351–1355.
O'Gorman, S., et al., 1997. Protamine-Cre recombinase transgenes efficiently recombine target sequences in the male germline of mice, but not in embryonic stem cells. Proc. Natl. Acad. Sci. U. S. A. 94, 14602–14607.
Popperl, H., Featherstone, M.S., 1993. Identification of a retinoic acid response element upstream of the murine Hox-4.2 gene. Mol. Cell. Biol. 13, 257–265.
Popperl, H., et al., 1995. Segmental expression of Hoxb-1 is controlled by a highly conserved autoregulatory loop dependent upon exd/pbx. Cell 81, 1031–1042.
Pratt, M.A., et al., 1993. Retinoic acid fails to induce expression of Hox genes in differentiation-defective murine embryonal carcinoma cells carrying a mutant gene for alpha retinoic acid receptor. Differentiation 53, 105–113.
Prince, V., Lumsden, A., 1994. Hoxa-2 expression in normal and transposed rhombomeres: independent regulation in the neural tube and neural crest. Development 120, 911–923.
Qin, P., et al., 2004a. Retinoic acid regulates the expression of PBX1, PBX2, and PBX3 in P19 cells both transcriptionally and post-translationally. J. Cell. Biochem. 92, 147–163.
Qin, P., et al., 2004b. Pre-B cell leukemia transcription factor (PBX) proteins are important mediators for retinoic acid-dependent endodermal and neuronal differentiation of mouse embryonal carcinoma P19 cells. J. Biol. Chem. 279, 16263–16271.
Raible, D.W., Eisen, J.S., 1996. Regulative interactions in zebrafish neural crest. Development 122, 501–507.
Ren, S.Y., et al., 2002. Targeted insertion results in a rhombomere 2-specific

Hoxa2 knockdown and ectopic activation of Hoxa1 expression. Dev. Dyn. 225, 305–315.

Rijli, F.M., et al., 1993. A homeotic transformation is generated in the rostral branchial region of the head by disruption of Hoxa-2, which acts as a selector gene. Cell 75, 1333–1349.

Rijli, F.M., et al., 1994. Insertion of a targeting construct in a Hoxd-10 allele can influence the control of Hoxd-9 expression. Dev. Dyn. 201, 366–377.

Robertson, E.J., et al., 1986. Germline transmission of genes introduced into cultured pluripotential cells by retroviral vector. Nature 323, 445–448.

Rudniki, M.A., McBurney, M.W., 1987. Cell culture methods and induction of differentiation of embryonal carcinom cell lines. In: Robertson, E.J. (Ed.), Teratocarcinomas and Embryonic Stem Cells, A Practical Approach. IRL Press, Oxford, pp. 19–49.

Saleh, M., et al., 2000. Cell signaling switches HOX–PBX complexes from repressors to activators of transcription mediated by histone deacetylases and histone acetyltransferases. Mol. Cell. Biol. 20, 8623–8633.

Schaeren-Wiemers, N., Gerfin-Moser, A., 1993. A single protocol to detect transcripts of various types and expression levels in neural tissue and cultured cells: in situ hybridization using digoxigenin-labelled cRNA probes. Histochemistry 100, 431–440.

Sechrist, J., et al., 1993. Segmental migration of the hindbrain neural crest does not arise from its segmental generation. Development 118, 691–703.

Serbedzija, G.N., et al., 1992. Vital dye analysis of cranial neural crest cell migration in the mouse embryo. Development 116, 297–307.

Simeone, A., et al., 1990. Sequential activation of HOX2 homeobox genes by retinoic acid in human embryonal carcinoma cells. Nature 346, 763–766.

Soriano, P., 1999. Generalized lacZ expression with the ROSA26 Cre reporter strain. Nat. Genet. 21, 70–71.

Studer, M., et al., 1996. Altered segmental identity and abnormal migration of motor neurons in mice lacking Hoxb-1. Nature 384, 630–634.

Thomas, K.R., Capecchi, M.R., 1987. Site-directed mutagenesis by gene targeting in mouse embryo-derived stem cells. Cell 51, 503–512.

Trainor, P.A., et al., 2002. Role of the isthmus and FGFs in resolving the paradox of neural crest plasticity and prepatterning. Science 295, 1288–1291.

Tybulewicz, V.L., et al., 1991. Neonatal lethality and lymphopenia in mice with a homozygous disruption of the c-abl proto-oncogene. Cell 65, 1153–1163.

Wakamatsu, Y., et al., 2000. Fate determination of neural crest cells by NOTCH-mediated lateral inhibition and asymmetrical cell division during gangliogenesis. Development 127, 2811–2821.

Wilkinson, K.D., et al., 1989. The neuron-specific protein PGP 9.5 is a ubiquitin carboxyl-terminal hydrolase. Science 246, 670–673.